REGGEIZATION OF SOME UNEQUAL MASS PROCESSES INVOLVING HIGHER SPINS: THE REACTIONS $\pi N \to VN$, $\pi N \to V\Delta$, and $\gamma p \to \pi^+ n$

Thesis by

Lorella Margaret Jones

In Partial Fulfillment of the Requirements

For the Degree of

Doctor of Philosophy

California Institute of Technology

Pasadena, California

1968

(Submitted November 9, 1967)

ACKNOWLEDGMENTS

The author would like to especially thank Professor Steven Frautschi, whose continued advice and encouragement inspired much of this work. She would also like to acknowledge helpful discussions with Dr. Ling-Lie Wang, Professor Murray Gell-Mann, and Drs. David Horn and Christoph Schmid.

Financial support by the National Science Foundation throughout the course of this work has been greatly appreciated.

ABSTRACT

Recent theoretical developments in the reggeization of inelastic processes involving particles with high spin are incorporated into a model of vector meson production. A number of features of experimental differential cross sections and density matrices are interpreted in terms of this model.

The method chosen for reggeization of helicity amplitudes first separates kinematic zeros and singularities from the parity-conserving amplitudes and then applies results of Freedman and Wang on daughter trajectories to the remaining factors. Kinematic constraints on helicity amplitudes at $t = 0$ and $t = (M - M_{\Delta})^2$ are also considered.

It is found that data for reactions of types $\pi N \to VN$ and $\pi N \to V\Delta$ are consistent with a model of this type in which all kinematic constraints at $t = 0$ are satisfied by evasion (vanishing of residue functions). As a quantitative test of the parametrization, experimental differential cross sections of vector meson production reactions dominated by pion trajectory exchange are compared with the theory. It is found that reduced residue functions are approximately constant, once the kinematic behavior near $t = (M - M_{\Delta})^2$ has been removed.

The alternative possibility of conspiracy between amplitudes is also discussed; and it is shown that unless conspiracy is present, some amplitudes allowed by angular momentum conservation will not contribute with full strength in the forward direction. An example, $\gamma p \to \pi^+ n$ in which the data for $d\sigma/dt$ indicate conspiracy, is studied in detail.

TABLE OF CONTENTS

Chapter 1

INTRODUCTION

Reggeization of vector meson production ($\pi B \rightarrow VB$, $\pi B \rightarrow V\Delta$) reactions and the related pion photoproduction reaction $\gamma p \rightarrow \pi^+ n$ has traditionally presented a number of problems. These may be divided into:

(a) Problems of principle, caused by unequal masses and the presence of high spins, and

(b) Problems of practice, among which we note especially the following:

i) The data for forward production of ρ mesons appear to be dominated by pi exchange at all energies despite the fact that the ω and A_2 trajectories have larger $\alpha(t)$'s.

ii) ω production differential cross sections and density matrices at small t bear scant resemblance to those predicted on the basis of ρ trajectory exchange, although this is the only well established trajectory which could contribute.

iii) For reactions such as ρ and f^o production, in which π exchange seems to dominate, a rapidly varying residue function is necessary to fit both the data and the known couplings at $t = m_\pi^2$.

iv) Standard reggeization techniques for various trajectories lead to the conclusion that there should be a dip in the

forward photoproduction cross section. It is well known, however, that at low energies the cross section has a peak at 0°, and there are experimental data at 2.5° cm which indicate this is still probably true at the highest energies measured (2-3 GeV/c = k_{γ}).

Recent developments in the Regge pole theory of unequal mass scattering[1] and the construction of helicity amplitudes free of kinematical singularities[2] now make possible a straightforward parametrization of inelastic reactions in which the particles have arbitrary spins and masses.[3] Within this framework, the Regge asymptotic form of a helicity amplitude is[3]

$$f^{t}_{cd;ab} = \frac{[1\pm e^{-i\pi\alpha(t)}]}{\sin \pi\alpha(t)} K(t) \left(\sin \frac{\theta_t}{2}\right)^{|\lambda-\mu|} \left(\cos \frac{\theta_t}{2}\right)^{|\lambda+\mu|} \bar{\gamma}(t) \left(\frac{s}{s_o}\right)^{\alpha-M}$$

where

$$\lambda = a-b \qquad \mu = c-d \qquad M = \max(|\lambda|, |\mu|) \ .$$

Here, K(t) is a known function of t containing kinematic singularities of the amplitude, and $\bar{\gamma}(t)$ is a smooth function of t.

This parametrization essentially solves all problems of principle, with the exception of relations among helicity amplitudes required by kinematical constraints at particular points (such as t = 0, thresholds, etc.). A method is now known for determining all such constraint equations.[4] Hence there are no longer fundamental mathematical obstructions to a thorough investigation of the applicability of Regge pole formalism in these reactions.

The purpose of this study is to demonstrate that the formalism outlined (i) provides an adequate basis for description of the particular reactions $\pi N \to VN$, $\pi N \to V\Delta$, $\gamma p \to \pi^+ n$, and (ii) allows solution in a natural way of many practical problems, including those listed above.

Chapter 2 is devoted to a discussion of the theoretical advances in reggeization of unequal mass processes, and processes containing high spin particles, which are applied in the rest of the work. In Chapter 3, a parametrization for reactions of the form $\pi B \to VB$, $\pi B \to V\Delta$ is developed and properties of this parametrization are related to features of the experimental density matrices and cross sections. Section 3.2 is devoted to the reggeization of pi exchange in these reactions; it is shown that the rapidly varying pi trajectory residue needed to fit differential cross section data can be understood as a kinematic rather than a dynamic phenomenon.

The analysis of Chapter 3 provides a great deal of evidence that conspiracy between trajectories is not important in vector meson production reactions. Nevertheless Chapter 4 is devoted to a theoretical examination of conspiracy relations in order to complete the kinematic discussion. It is demonstrated that the option of conspiracy plays an important role by allowing all angular-momentum conserving s-channel amplitudes to contribute in principle in the forward direction. As an example of a related reaction in which conspiracy does seem necessary to account for experimental observations, the reaction $\gamma p \to \pi^+ n$ is discussed in Chapter 5.

Chapter 2

BASIC THEORY

2.1 Method of Reggeization

For elastic scattering of spinless particles, the contribution of the leading Regge pole, obtained from a Sommerfeld-Watson transformation on the amplitude, takes the form

$$\bar{\beta}(t) \left[\frac{1 \pm e^{-i\pi\alpha(t)}}{\sin \pi\alpha(t)}\right] (q_t\, k_t)^{\alpha(t)} \; P_\alpha(\cos \theta_t) \qquad \text{(II.1)}$$

where

$$\cos \theta_t = \frac{s}{2q_t k_t} + \frac{t - 2(m_a^2 + m_c^2)}{4\, q_t\, k_t} \; . \qquad \text{(II.2)}$$

As $s \to \infty$, $(q_t\, k_t)^{\alpha(t)}\; P_\alpha(\cos \theta_t) \to s^{\alpha(t)}$. Thus, in this case, those trajectories with the highest $\alpha(t)$ should dominate, regardless of the value of (negative) t.

For processes in which the external masses at a single vertex are unequal (Fig. II.1),

$$\cos \theta_t = \frac{2t\,(s - m_a^2 - m_c^2) + (t + m_a^2 - m_b^2)\,(t + m_c^2 - m_d^2)}{\left\{[t-(m_a-m_b)^2][t-(m_a+m_b)^2][t-(m_c-m_d)^2][t-(m_c+m_d)^2]\right\}^{1/2}} \qquad \text{(II.3)}$$

At $t = t_{min}$, $\cos \theta_t = -1$. Within a region about t_{min}, often referred to as the forward cone, $|\cos \theta_t|$ is small and the replacement of $P_\alpha(\cos \theta_t)$ by $(\cos \theta_t)^\alpha$ is no longer justified. In other words, when the external masses at a single vertex are unequal, it is no longer

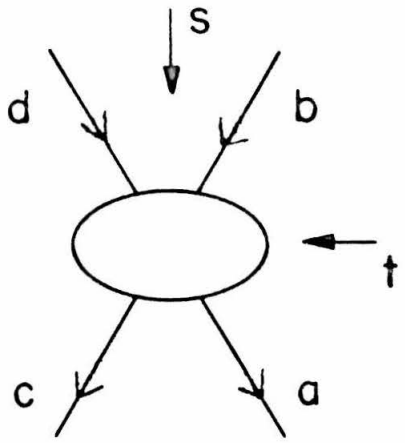

Figure II.1

Labeling of Particle Kinematics

clear which term in the expansion in powers of s of $(q_t\ k_t)^{\alpha(t)}\ P_\alpha(\cos\theta_t)$ dominates at low t. The ambiguity has been resolved in the spinless case by the work on daughter trajectories,[1] which demonstrates that those terms in the expansion which are singular at t = 0 will be cancelled by the contributions of the daughters. Hence the $s^{\alpha(t)}$ behavior of the Regge pole contribution is preserved, and the resulting amplitude contains only singularities of a dynamical nature.

When the external particles have spin, some care must be used in applying the above method. In order to carry through the procedure, it was necessary to write the invariant amplitude for the process in the form of a dispersion integral with the location of the cuts and the discontinuities across them determined solely by the dynamics of the process. Thus a major problem in the case with spin is to determine which pieces of the physical amplitude can be expressed in this manner. It is most convenient to find expressions closely related to the t-channel helicity amplitudes, as the differential cross section and the density matrices can all be expressed simply in terms of these. It has been found[2] that if $f_{cd;ab}$ is the t-channel helicity amplitude for the problem, defined by

$$\langle p_c,\ c;\ p_d,\ d\ |S - 1|\ p_a, a;\ p_b,\ b\rangle$$
$$= i\ (2\pi)^4\ \delta(p_c + p_d - p_a - p_b)\ f_{cd;ab}\ [p_a^{\,o}\ p_b^{\,o}\ p_c^{\,o}\ p_d^{\,o}]^{-1/2} \qquad (II.4)$$

and

$$\bar{f}_{cd;ab} = f_{cd;ab} \Big/ \left(\sin\frac{\theta_t}{2}\right)^{|\lambda-\mu|} \left(\cos\frac{\theta_t}{2}\right)^{|\lambda+\mu|} \qquad \text{(II.5)}$$

where $\lambda = a-b$, $\mu = c-d$, then

$$\bar{f}^t_{cd;ab} \pm \bar{f}^t_{-c-d;ab} = K^{\pm}(t)\ \tilde{f}^{\pm}(s,t) \quad , \qquad \text{(II.6)}$$

where $K(t)$ is determined by methods discussed in the following section, and $\tilde{f}^{\pm}(s,t)$ is analytic except for dynamical singularities. $\tilde{f}$ may then be written in the form of a dispersion integral and the application of methods similar to those used in the case of unequal mass spinless scattering yields an asymptotic form.[5] The result is that $\tilde{f}$ takes the form

$$\bar{\gamma}^{\pm}(t)\ \ s^{\alpha-M}\ \ \left[\frac{1 \pm e^{-i\pi\alpha(t)}}{\sin\pi\alpha(t)}\right]$$

where $M = \max(|\lambda|, |\mu|)$ and $\bar{\gamma}^{\pm}(t)$ is expected to be a smooth function of t. Hence the s-dependence of each $f_{cd;ab}$ arises from two sources: (i) the factor $\tilde{f}$, in which the $s^{\alpha-M}$ behavior is preserved by contributions of daughter trajectories; and (ii) the kinematic factors $(\sin\theta_t/2)^{|\lambda-\mu|}\ (\cos\theta_t/2)^{|\lambda+\mu|}$. At large t, these kinematic factors contribute the remaining s^M, but in the "cone" at low t this growth is suppressed when the masses are unequal.

To place these conclusions for helicity amplitudes on the same intuitive basis as those for spinless scattering, it is helpful to examine some of the details involved in the replacement of

$\bar{f}^t_{cd;ab} \pm \bar{f}^t_{-c-d;ab}$ by

$$K^{\pm}(t)\ \bar{\gamma}^{\pm}(t)\ s^{\alpha-M}\ [1 \pm e^{-i\pi\alpha(t)}]/\sin \pi\alpha(t)$$

for a particular exchange. Because of the action of the parity operator on helicity states[6]

$$\mathcal{P}\ |J,\ \lambda_1,\ \lambda_2\rangle = \eta_1\eta_2(-1)^{J-s_1-s_2}\ |J,\ -\lambda_1,-\lambda_2\rangle \qquad \text{(II.7)}$$

a Regge pole of parity P will couple to the particular linear combination of vector-pseudoscalar meson states $|J,\lambda_1\lambda_2\rangle + (-1)^{J+1}P|J,-\lambda_1-\lambda_2\rangle$ (where P is either $(-1)^J$ or $(-1)^{J+1}$). Thus its contribution to the partial wave amplitude obeys $T^J_{-c-d;ab}(t) = P(-1)^{J+1}\ T^J_{cd;ab}(t)$, and hence for exchange of a spin J object

$$\bar{f}^t_{cd;ab} \pm \bar{f}^t_{-c-d;ab} = \sum_J T^J_{cd;ab} \left[\frac{d^J_{\lambda\mu}(\theta)}{\left(\sin\frac{\theta_t}{2}\right)^{|\lambda-\mu|}\left(\cos\frac{\theta_t}{2}\right)^{|\lambda+\mu|}} \pm \frac{P(-1)^{J+1}\ d^J_{\lambda-\mu}(\theta)}{\left(\sin\frac{\theta_t}{2}\right)^{|\lambda+\mu|}\left(\cos\frac{\theta_t}{2}\right)^{|\lambda-\mu|}} \right] . \qquad \text{(II.8)}$$

Expansion of the $d^J_{\lambda\mu}(\theta)$ in powers of $\cos\theta_t$ shows that a given Regge pole contributes with maximum strength to only one of the amplitudes (II.8); its contribution to the other amplitude is proportional to a smaller power of s. For large s, therefore, if the contribution is mainly to the (±) amplitude, $\bar{f}^t_{cd;ab} \approx (\pm)\ \bar{f}^t_{-c-d;ab}$. To determine

whether the important amplitude is the sum or the difference, it is convenient to use the properties

$$d^J_{\lambda\mu}(\theta) = (-1)^{\lambda-\mu}\, d^J_{\mu\lambda}(\theta) = (-1)^{\lambda-\mu}\, d^J_{-\lambda-\mu}(\theta) \qquad \text{(II.9)}$$

to obtain

$$d^J_{\lambda\mu} = e^{i\varphi_1}\, d^J_{\lambda_1\lambda_2}(\theta) \quad ; \quad d^J_{\lambda-\mu} = e^{i\varphi_2}\, d^J_{\lambda_3\lambda_4}(\theta)$$

where φ_1, φ_2, and the λ_i's are defined by the requirement that $\lambda_1 + \lambda_2$, $\lambda_1-\lambda_2$, $\lambda_3+\lambda_4$, and $\lambda_3-\lambda_4$ all be greater than or equal to 0. For $d^J_{\lambda_1\lambda_2}$ functions in which the indices have this property,

$$d^J_{\lambda_i\lambda_j} = \left(\sin\frac{\theta_t}{2}\right)^{\lambda_i-\lambda_j} \left(\cos\frac{\theta_t}{2}\right)^{\lambda_i+\lambda_j} P^{(\lambda_i-\lambda_j,\ \lambda_i+\lambda_j)}_{J-M}(\cos\theta_t) \ ; \qquad \text{(II.10)}$$

hence,

$$\bar{f}^t_{cd;ab} \pm \bar{f}^t_{-c-d;ab} = \sum_J T^J_{cd;ab} \left[e^{i\varphi_1}\, P^{(|\lambda-\mu|,\ |\lambda+\mu|)}_{J-M}(\cos\theta_t) \pm P\,(-1)^{J+1}\, e^{i\varphi_2}\, P^{(|\lambda+\mu|,\ |\lambda-\mu|)}_{J-M}(\cos\theta_t) \right] \qquad \text{(II.11)}$$

and the amplitude with the most important contribution has sign $(\pm)$ if $e^{i(\varphi_2-\varphi_1)}\,(-1)^{J+1}\,P$ is $(\pm)$.

Systematic application of the method of Ref. 5 shows that $\gamma_\pm(t)$ contains functions of $\alpha(t)$. These are not important except at those places where they require the amplitude to vanish; in general, an amplitude derived from $d^J_{\lambda\mu}$ must vanish for all integer J smaller than $|\lambda|$ or $|\mu|$. In vector meson production at low negative t, this

means that all $P = (-1)^J$ exchanges (which have $|\mu| = 1$, $M \geq 1$ as shown in Section 3.1) must vanish at $\alpha = 0$. Because $\alpha = 0$ occurs for $|t| \gtrsim 0.5$ GeV^2 for the ρ, ω, and A_2 exchanges considered here, this effect may be considered independently of forward kinematic effects and is not of central interest to this study.

For our purposes, the important thing to notice is the form

$$f_{cd;ab} = g(t) \left(\sin \frac{\theta_t}{2}\right)^{|\lambda-\mu|} \left(\cos \frac{\theta_t}{2}\right)^{|\lambda+\mu|} s^{\alpha(t)-M} . \tag{II.12}$$

At the lowest physical $|t|$ for the s-channel process, $\cos \theta_t \to -1$, $\cos \frac{\theta_t}{2} \to 0$. Also, $(d \cos \theta_t)/ds \to 0$ as $t \to 0$ for any unequal mass process. For such low $|t|$, therefore, the s-dependence of the amplitude is reduced by the maximum helicity in the t-channel, M. If for some reason the trajectory with largest $\alpha(t)$ cannot have $M = 0$, a lower trajectory may account for the observations at small $|t|$. This is exactly what happens in vector meson production.

In order to distinguish between the simple cone effect ($|\cos \theta_t| \sim 1$) due only to unequal masses, and this effect (which depends also on a particular treatment of the spin kinematics), the reduction in power of s will be referred to as spin suppression.

2.2 Identification of Kinematic Singularities and Zeros

The discussion above assumed that amplitudes $\tilde{f}^{\pm}(s,t)$, analytic except for dynamical singularities, could be obtained by a particular procedure. In the following paragraphs, this procedure

is justified and the method used to obtain $K^{\pm}(t)$ is explained.

Helicity amplitudes f^t contain various "kinematic" zeros and singularities, which are fixed by angular momentum requirements. Once these are identified and factored out, the remaining factors will have only dynamical singularities, with resulting simplifications in the representation of Regge residues. The first step in this direction was taken by Gell-Mann et al.,[5] who isolated the kinematic zeros which occur at forward and backward scattering angles in the t-channel. For

$$f^t_{cd;ab} = (\sin\frac{\theta_t}{2})^{|\lambda-\mu|} \quad (\cos\frac{\theta_t}{2})^{|\lambda+\mu|} \bar{f}^t_{cd;ab} \qquad \text{(II.13)}$$

the kinematic factor $(\sin\frac{\theta_t}{2})^{|\lambda-\mu|}$ vanishes like $\theta_t^{|\lambda-\mu|}$ in the forward direction; this expresses the fact that conservation of angular momentum along the direction of forward scattering requires helicity conservation, $\lambda = \mu$ (otherwise, the amplitude must vanish). Similarly, the kinematic factor

$$(\cos\frac{\theta_t}{2})^{|\lambda+\mu|}$$

vanishes like $(\pi - \theta_t)^{|\lambda+\mu|}$ in the backward direction; this expresses the fact that conservation of angular momentum along the direction of backward scattering requires the helicity to reverse sign, $\lambda = -\mu$.

The remaining factor $\bar{f}^t$ has the partial wave expansion

$$\bar{f}^t_{cd;ab} = \Sigma_J \, (2J+1) \, F^J_{cd;ab}(t) \, P^{(|\lambda-\mu|,\ |\lambda+\mu|)}_{J-M}(\cos\theta_t) \qquad \text{(II.14)}$$

where

$$M = \text{maximum of } (|\lambda|,\ |\mu|)$$

and P_{J-M} is a Jacobi polynomial. Since the remaining $\cos\theta_t$ dependence in $\bar{f}^t$ is a sum over polynomials which are non-singular at finite $\cos\theta_t$, and are not all zero at the same $\cos\theta_t$,[7] and since

$$\cos\theta_t = \frac{[2\,s\,t + t^2 - t\,\Sigma_i\, m_i^2 + (m_a^2 - m_b^2)\,(m_c^2 - m_d^2)]}{\sqrt{(t-(m_a+m_b)^2)\,(t-(m_a-m_b)^2\,(t-(m_c+m_d)^2)\,(t-(m_c-m_d)^2)}} \qquad \text{(II.15)}$$

is linear in s, $\bar{f}^t$ has no further kinematic singularities or zeros in $\cos\theta_t$ or s.

The remaining problem is to factor out of $\bar{f}^t$ the kinematic singularities and zeros in the other variable, t. We know there are such singularities from any of the following methods:

(i) study of Feynman diagrams;

(ii) study of behavior at t-channel thresholds;

(iii) relating f^t to f^s by crossing, and noting that f^s has kinematic singularities in $\cos\theta_s$ (i.e., in t) and that the crossing matrix has further singularities in t.

Hara[8] studied the singularities by a combination of all three methods, while Wang[2] used the crossing method exclusively. In either case, it proved most convenient to consider the "parity-conserving" combinations $\bar{f}^t_{cd;ab} \pm \bar{f}^t_{-c-d;ab}$, and Hara and Wang split these into a kinematic factor $K^{\pm}$ and a dynamical factor $\tilde{f}$:

$$\bar{f}^{t}_{cd;ab} \pm \bar{f}^{t}_{-c-d:ab} = K^{\pm}_{cd;ab}(t) \quad \tilde{f}^{\pm t}_{cd;ab}(t,s) \quad , \qquad \text{(II.16)}$$

giving a prescription for $K^{\pm}$.

In detail, the crossing method makes use of

$$f^{t}_{i} = \sum_{j} X_{ij} \, f^{s}_{j} \qquad \text{(II.17)}$$

where the subscript i stands for the set of helicity states cd, ab, and X_{ij} is the crossing matrix explicitly given by Trueman and Wick.[9] The corresponding relation for the $\bar{f}$'s is

$$\bar{f}^{t}_{i} = \sum_{j} \bar{X}_{ij} \, \bar{f}^{s}_{j} \qquad \text{(II.18)}$$

where

$$\bar{X}_{ij} = \frac{X_{ij} \, (\sin\frac{\theta_s}{2})^{|\lambda'-\mu'|} \, (\cos\frac{\theta_s}{2})^{|\lambda'+\mu'|}}{(\sin\frac{\theta_t}{2})^{|\lambda-\mu|} \, (\cos\frac{\theta_t}{2})^{|\lambda+\mu|}} \qquad \text{(II.19)}$$

and λ' and μ' are the incoming and outgoing helicities in the s-channel center-of-mass system. The kinematic singularities and zeros of $\bar{f}^{t}$ in t are all in the explicitly known $\bar{X}$, since $\bar{f}^{s}$ has none. Thus by careful examination of $\bar{X}$, Wang was able to obtain a prescription for the kinematic singularities which is, as far as we know, complete. Wang's prescription for the $K^{\pm}$ is used throughout this work; this is all that is needed for the discussion in Section 2.1.

The amplitudes $\tilde{f}^{\pm}(s,t)$ identified in Eq. (II.6) are, however, subject to further kinematic constraints. This is because the

program outlined, as implemented by Hara and Wang, was not completed; kinematic zeros remain in linear combinations of $\tilde{f}$'s.[4,10,11] For example, if one takes Wang's singularity-free amplitudes $\tilde{f}^t_i$ for $NN \to NN$, it turns out they are not all linearly independent at $t = 0$ and $t = 4M^2$. Thus there are linear combinations of the $\tilde{f}^t_i$ which have kinematic zeros at these points. In terms of the equation

$$\tilde{f}^t_i = \sum_j \tilde{X}_{ij} \bar{f}^s_j \qquad \text{(II.20)}$$

this implies that the different rows of $\tilde{X}_{ij}$ are not all independent; i.e., the determinant of $\tilde{X}_{ij}$ has zeros and the linear combinations of $\tilde{f}^t_i$ which vanish are the eigenvectors associated with the zero eigenvalues of $\tilde{X}$. The reason Wang's study is incomplete, then, is that it is not enough to locate the singularities and zeros in <u>each row</u> of the matrix $\bar{X}_{ij}$; one must also locate the extra zeros of the <u>determinant</u> of $\tilde{X}_{ij}$.[12]

Of course, one can work out the determinant of $\tilde{X}$ by hand and locate its zeros explicitly in any particular case, but it would be much more convenient to have a general prescription for the answer. Fox[10] has given such a prescription for the class of reactions in which at least two particles are spinless. More recently, Cohen-Tannoudji, Morel, and Navelet[4] have pointed out that at zeros of det $\tilde{X}$, elements of the inverse matrix $\tilde{X}^{-1}$ which appears in

$$\bar{f}^s_i = \sum_j \tilde{X}^{-1}_{ij} \tilde{f}^t_j \qquad \text{(II.21)}$$

will have poles, and it is easier to locate poles than to form a determinant.[13] If the matrix elements of $\tilde{X}^{-1}_{ij}$ have the form

$$\tilde{X}^{-1}_{ij} = \frac{c_{ij}}{t-t_o} + (\text{terms regular at } t_o) \quad , \qquad (II.22)$$

then the condition

$$\sum_j c_{ij} \tilde{f}^t_j (t_o) = 0 \qquad (II.23)$$

must hold, since neither $\bar{f}^s_i$ nor the individual elements $\tilde{f}^t_j$ have kinematic singularities or zeros at $t = t_o$.

The physical nature of the additional kinematic zeros may be guessed from NN scattering. In this example, the conditions at $t = 4M^2$ are those expected at threshold due to the dominance of ${}^3(\ell = J-1)_J$ over ${}^3(\ell = J+1)_J$ states at this point.[14] For the meson production reactions studied here, the additional kinematic zeros again have the physical interpretation of threshold and pseudothreshold conditions at $t = (m_a \pm m_b)^2$, $t = (m_c \pm m_d)^2$. It is these extra threshold and pseudothreshold zeros which provide the relations used in discussing pion exchange (Section 3.2).

Kinematic conditions also occur at $t = 0$; these "conspiracy relations" are especially important to the study of forward scattering processes. In the example of NN scattering, a physical interpretation may be given the relation by noticing that $t = 0$ coincides with $\theta_s = 0^o$. At this point the vanishing of s-channel amplitudes $f^s_{c'd';a'b'}$ like $t^{|\lambda'-\mu'|/2}$ for $\lambda' = a'-b'$, $\mu' = c'-d'$ due to angular momentum conservation yields directly through crossing the

well-known conspiracy relation $f^t_{++;++} - f^t_{++;--} = f^t_{+-;+-} - f^t_{+-;-+}$. When the masses in either or both the initial and final states of the t-channel reaction are unequal, the point t = 0 is no longer physical (except in the limit $s \to \infty$). It is thus less easy to see intuitively that additional conditions should exist, although Bardakci and Segre[15] have given a method by which the additional symmetry at t = 0 in these reactions can be displayed from a physical point of view. Application of the method of Cohen-Tannoudji et al. leads, however, in a natural fashion to conspiracy conditions on the $\tilde{f}^t$ comparable to those on the f^t found in equal mass processes (see Appendix A). Physical consequences of these are discussed in Chapter 4 for the reactions in question.

Chapter 3

APPLICATION TO DATA OF THE NO-CONSPIRACY PARAMETRIZATION FOR $\pi N \to VN$, $\pi N \to V\Delta$

3.1 Parametrization of the Reactions

The purpose of this section is to examine the qualitative effects which kinematic factors may produce at small $|t|$ in differential cross sections and density matrix elements of vector meson production reactions. Three different types of factors are considered: half-angle factors, the Wang K(t), and additional powers of t suggested by physical considerations such as factorization of Regge residues. For all cases of importance (see below), the factors found this way for single trajectory exchange have the t = 0 behavior required by an evasive solution to the conspiracy relations listed in Chapter 4; thus this may be considered a study of the no-conspiracy case.

A Kinematic Peculiarity of Vector Meson Production

Application of the parity operator to a pion-vector meson helicity state gives

$$\mathcal{P} \; |J\ m;\ \lambda 0> = \; (-1)^{J+1} \; |J\ m;\ -\lambda\ 0> \qquad \text{(III.1)}$$

Thus the state in which the vector meson has helicity 0 can couple only to systems with "unnatural parity," $P = (-1)^{J+1}$. (This will be true for the production by pseudoscalar mesons of any system with "natural" parity, $P = (-1)^{S}$). Hence, M = 1 is the smallest value of M possible for exchange of a Regge trajectory with $P = (-1)^{J}$. [16]

Due to the form of the reggeized amplitude (Eq. II.12) and the low t behavior of the half angle factors $\cos \frac{\theta_t}{2}$ and $\sin \frac{\theta_t}{2}$, exchanges with $P = (-1)^J$ will effectively be suppressed by at least a power of s in the forward direction. This means that in any reaction where the pi trajectory is the $P = (-1)^{J+1}$ exchange with highest α, its contribution can dominate the cross section at large s and sufficiently small t despite the possibility of natural parity exchanges with higher-lying trajectories. More generally, the effect will enhance the relative importance of M = 0 amplitudes in the forward direction even in cases where known exchanges have $P = (-1)^J$. For larger t, the $\sin \frac{\theta_t}{2}$ and $\cos \frac{\theta_t}{2}$ terms are proportional to $s^{1/2}$; thus for large enough t and s, the normal hierarchy of trajectories should be seen.

Effects of $\bar{K}(t)$

Without examining the other pieces of the amplitude in detail, we have pinpointed a possible explanation for the experimental observation that pseudoscalar exchange tends to dominate the most forward directions in any vector meson production reactions in which it is possible, while natural parity exchanges become more important at larger t.[17] The $(\sin \theta_t/2)^{|\lambda-\mu|}$ $(\cos \theta_t/2)^{|\lambda+\mu|}$ pieces contain, of course, only a portion of the t-dependence of the amplitude. To be able to say that natural parity exchanges are kinematically suppressed at low t, one must make certain that K(t) does not tend to cancel the half angle effects. To this end, $\bar{K}(t)$ has been listed for the cases of interest. (Table III.1)

Table III.1

Kinematic Factors $\bar{K}(t)$ for Helicity Amplitudes

In this table $\lambda = \lambda_{N'} - \lambda_N$; $\mu = \lambda_V$; $N' = N, \Delta$

$$\tau_{\pi V} = [(t - (m_V - m_\pi)^2)(t - (m_V + m_\pi)^2)]^{\frac{1}{2}} .$$

$\pi B \to VB$

μ	λ	K(t) Solely From Crossing Matrix	From Factorization of Residues	Net
$P=(-1)^{J+1}$				
0	0	$t^{-\frac{1}{2}}\tau_{\pi V}^{-1}$	$t(\pi$ trajectory)	$t^{\frac{1}{2}}\tau_{\pi V}^{-1}$
1	0	$(t-4M^2)^{\frac{1}{2}}t^{-\frac{1}{2}}$	$t(\pi$ trajectory)	$t^{\frac{1}{2}}(t-4M^2)^{\frac{1}{2}}$
0	1	$(t-4M^2)^{\frac{1}{2}}t^{-\frac{1}{2}}$		$(t-4M^2)^{\frac{1}{2}}t^{-\frac{1}{2}}$
1	1	$(t-4M^2)^{\frac{1}{2}}$		$(t-4M^2)^{\frac{1}{2}}$
$P=(-1)^{J}$				
1	0	$\tau_{\pi V}$		$\tau_{\pi V}$
1	1	$\tau_{\pi V}t^{-\frac{1}{2}}$	t	$t^{\frac{1}{2}}\tau_{\pi V}$

$\pi B \to V\Delta$

All Factors Come from Crossing Matrix

$P=(-1)^{J+1}$		
0	0	$\tau_{\pi V}^{-1}[t - (M+M_\Delta)^2]^{-1}[t - (M-M_\Delta)^2]^{-\frac{1}{2}}$
0	1	$t^{-\frac{1}{2}}[t - (M+M_\Delta)^2]^{-\frac{1}{2}}$
0	2	$\tau_{\pi V}[t - (M-M_\Delta)^2]^{\frac{1}{2}}t^{-1}$
1	0	$t^{-\frac{1}{2}}[t - (M+M_\Delta)^2]^{-\frac{1}{2}}$
1	1	$[t - (M+M_\Delta)^2]^{-\frac{1}{2}}$
1	2	$\tau_{\pi V}[t - (M-M_\Delta)^2]^{\frac{1}{2}}t^{-\frac{1}{2}}$
$P=(-1)^{J}$		
1	0	$\tau_{\pi V}t^{-\frac{1}{2}}[t - (M-M_\Delta)^2]^{-\frac{1}{2}}$
1	1	$\tau_{\pi V}[t - (M-M_\Delta)^2]^{-\frac{1}{2}}$
1	2	$(\tau_{\pi V})^2\, t^{-\frac{1}{2}}[t - (M+M_\Delta)^2]^{\frac{1}{2}}$

Clearly, all threshold factors and the vector-pseudoscalar pseudothreshold ($[t-(m_V-m_\pi)^2]^{1/2}$) factors will be smooth enough in the region of small negative t to be absorbed into $\gamma(t)$. The only portions of K(t) which might be important at low t are factors of $t^{1/2}$ and of $[t-(M_N-M_\Delta)^2]^{1/2}$. From Table III.1, one sees that the dominant amplitudes for both types of parity exchange contain the same $N\bar{\Delta}$ pseudothreshold factor, $[t-(M-M_\Delta)^2]^{-1/2}$. Hence this factor can be neglected in the study of relative enhancement; the only parts of K(t) which might compete with the spin suppression effects are powers of $t^{1/2}$. Most of those listed in Table III.1 fall into three categories:

i) Factor of $t^{1/2}$ in the π exchange $\lambda = 0, \mu = 0$ amplitude for $\pi B \to VB$ found by factorization of residues.

At first glance, one might expect this to be comparable to the cos $\theta_t/2$ terms which appear in natural parity exchanges. However, the π exchange amplitude is strongly affected by the π pole, so that the overall behavior at small t may be approximated by $\sqrt{t/t-\mu^2}$ which suppresses the amplitude only for $|t| < 0.02$ GeV^2.

In contrast, the poles for natural parity exchanges do not have much effect on the amplitudes, and the effects of spin suppresion are appreciable out to $|t| \approx 0.2$ GeV^2. [18] Hence, for the range $0.02 \leq |t| \leq 0.2$ GeV^2, the π exchange can be expected to dominate natural parity exchanges.[19]

ii) Factors of $t^{-1/2}$ in $\pi B \to V\Delta$ reactions.

In reactions where the masses are related as in $\pi B \to V\Delta$,

$\sin \theta_t/2$ behaves near t = 0 like $\sqrt{t}$. (In contrast, for $\pi B \to VB$, $\sin \theta_t/2 \sim 1/\sqrt{2}$ near t = 0.) Because of this behavior, each parity-conserving combination $\bar{f}_{cd;ab} \pm \bar{f}_{-c-d;ab}$ has a kinematic factor $t^{-\xi/2}$, $\xi = \max(|\lambda-\mu|, |\lambda+\mu|)$.[2,8)]

It happens, however, that when cross sections are formed in a single Regge pole model, these amplitudes contribute only the factor $(\sin \theta_t/2)^{2\xi'}$, where $\xi' = \min(|\lambda-\mu|, |\lambda+\mu|)$. Thus in order to remove kinematic zeros in the cross section, it is necessary to have only a kinematic factor of $t^{-\xi'/2}$ from each of the amplitudes. This is the factor which appears in Table III.1. It follows from the above discussion that these factors do not make the amplitude increase at small t (because they are cancelled by the t = 0 zero in $(\sin \theta_t/2)$, neither do they cancel the zero in $\cos \theta_t/2$ due to the cone effect.

iii) Factors of $t^{1/2}$ in the $P = (-1)^J, |\lambda| = 1, |\mu| = 1$ and $P = (-1)^{J+1}, |\mu| = 1, \lambda = 0$ amplitudes for $\pi B \to VB$.

These are implied by the factorization condition when the kinematic singularity $(1/\sqrt{t})^{\min(|\lambda-\mu|, |\lambda+\mu|)}$ justified in (ii) is used for the $\pi\pi \to VV$ amplitude.

Hence, for single Regge pole models, none of the kinematic factors in K(t) will cancel the spin suppression effect in the region $0.02 \leq |t| \leq 0.2$ GeV^2.[20)] The $t^{1/2}$ factors are the kinematic factors which have the greatest effect on the behavior in the region of interest; thus, for purposes of fitting, the amplitudes may be approximated by the form

$$h(t)\ f(t^{\frac{1}{2}})\left[\frac{1\pm e^{-i\pi\alpha(t)}}{\sin\ \pi\alpha(t)}\right](\sin\frac{\theta_t}{2})^{|\lambda-\mu|}(\cos\frac{\theta_t}{2})^{|\lambda+\mu|}\left(\frac{s}{s_o}\right)^{\alpha(t)-M} \qquad \text{(III.2)}$$

where $f(t^{\frac{1}{2}})$ is found in Table III.1, and h(t) is more slowly varying.

A number of comments about this parametrization are in order:

a) In both types of reactions considered, the product of kinematic factors $K(t)\ (\sin\theta_t/2)^{|\lambda-\mu|}(\cos\theta_t/2)^{|\lambda+\mu|}$, when evaluated in the physical region of the s-channel, has the same phase (up to a sign) for all helicity amplitudes corresponding to a given trajectory. This means that relative phases between helicity amplitudes are determined solely by the $\gamma(t)$'s.

b) The entire residue takes the form $K(t)\ (P_{\pi V}\cdot P_{NN'})^{\alpha-M}\gamma(t)$. Near each fermion-antifermion threshold, it is observed to have the behavior (Ref. 3, footnote 8)

$$(t-4M^2)^{L_i} \qquad \text{or} \qquad [t-(M+M_\Delta)^2]^{L_i}$$

where L_i is the smallest permissable orbital angular momentum for the parities and spins involved.

Near the pseudothreshold $t = (M-M_\Delta)^2$ it has the behavior $[t-(M-M_\Delta)^2]^{L'}$ where L' is the lowest possible orbital angular momentum for a pair of fermions with intrinsic parity +. In other words, the pseudothreshold behavior is the same as threshold behavior for a particle with negative mass and opposite parity to one of the fermions.

The behavior at the boson threshold is normal and is identical to that at the pseudothreshold. Presumably this is because the antibosons have the same parities as the bosons.

c) As we are approximating all amplitudes by Regge poles, the residues $K(t)\bar{\gamma}(t)\ (P_{\pi V}\ P_{NN'})^{\alpha-M}$ must obey the factorization condition. This places additional constraints on the analytic pieces $\gamma(t)$.[3] The additional powers of t discussed above are the minimum required by the comparison

$$\left[\beta^{\pi N \to VN}_{\lambda,\mu}\right]^2 = \beta^{\pi\pi \to VV}_{\mu,\mu}\ \beta^{NN \to NN}_{\lambda,\lambda}$$

(provided the factor $(1/\sqrt{t})^{\min(|\lambda-\mu|, |\lambda+\mu|)}$ is used in computing $\beta^{\pi\pi \to VV}$). This provides information only at $t = 0$, as all the residues automatically have the proper behavior at thresholds.

d) The kinematic factors obtained from crossing matrix and factorization considerations agree with those found by considering all perturbation theory graphs for the exchange.[21]

e) The kinematical factors in Table III.1 are (with the exception of the $|\lambda| = 1$, $\mu = 0$ amplitude of $\pi B \to VB$, as explained in Ref. 21)) those which would apply in the case of a single Regge pole exchange, i.e., when only one parity-conserving helicity amplitude is important to highest power of s. This situation may be characterized by the requirement that all subsidiary conditions[4] imposed on the helicity amplitudes by kinematics at $t = 0$ are satisfied by the vanishing of individual regularized helicity amplitudes at this point, rather than by conspiracy between amplitudes.

Removal of this requirement would allow the amplitudes for $\pi B \to V\Delta$ and $\pi\pi \to VV$ to have a singularity of order $(1/\sqrt{t})^{|\lambda|+|\mu|}$; also, the additional t's listed for some $\pi B \to VB$ amplitudes would not be required. The coefficients of the singular terms would in this case have to satisfy conspiracy relationships. In the s-channel physical region, the resulting singularities of the $|\lambda| = |\mu|$ helicity amplitudes would cancel the spin suppression dip due to half angle factors, and there would be no kinematic reason for $P = (-1)^{J+1}$ dominance of the forward peak (see Chapter 4). However, all the experimental evidence to date on vector meson production is consistent with the no-conspiracy hypothesis; hence, we conclude that any contributions actually containing the additional singularities are small enough to be neglected in these reactions. This is the point of view taken in the analysis in the following section.

Relations between the amplitudes at points other than $t = 0$ (thresholds and pseudothresholds) have not been considered in this section.

Application to Data

For the purpose of illustration, we consider only the reactions $\pi N \to \omega N$, $\pi N \to \rho N$, $\pi N \to \omega\Delta$, and $\pi N \to \rho\Delta$ because the number of possible exchanges in these is sharply limited by G parity and isospin. Identical kinematic statements can be made about the processes $KN \to K^*N$, $KN \to K^*\Delta$; the density matrices and differential cross sections for these reactions have the same qualitative behavior as those for ρ production.[22)]

The differential cross section for production of ρ mesons, both with and without an isobar, possesses a well-defined diffraction peak at all energies in the range 2.5 - 8 GeV/c incident pion momentum.[23,24,25] The spin density matrices of the ρ's produced closely resemble those for elementary one-pion exchange ($\rho_{00} = 1$; Re $\rho_{10} = 0$, $\rho_{1-1} = 0$) at the lowest physical t, but as t increases the value of ρ_{00} decreases and that of ρ_{1-1} increases.[25] This makes the density matrices look somewhat more like those expected from elementary vector meson exchange (ρ_{00} = Re $\rho_{10} = 0$).

Trajectories which may be exchanged in this reaction are π, A_2(R), and ω (in non-charge-exchange $\pi N \to \rho N$). As the A_2 and ω have natural parity, it is expected that they will be suppressed at small t and that the forward peak is produced by π exchange. In fact, the region $0.05 \leq |t| \leq 0.4$ GeV^2 agrees fairly well with an amplitude of the form

$$\pi N \to VN \qquad \sqrt{t}\, g(t)\, [1 + e^{-i\pi\alpha_\pi(t)}]\, (s/s_o)^{\alpha_\pi(t)} / \sin \pi\alpha_\pi(t) \ ,$$

$$\pi N \to V\Delta \qquad \bar{g}(t)\, [1 + e^{-i\pi\alpha_\pi(t)}]\, (s/s_o)^{\alpha_\pi(t)} / \sin \pi\alpha_\pi(t) \ , \tag{III.3}$$

over the experimental range of s (see Section 3.2). Deviations from this at larger t become more pronounced at the higher energies, as expected (the region over which suppression is appreciable decreases as the energy increases).[18,26]

In contrast, the differential cross section for production of ω mesons is quite flat as a function of t at all energies measured.[23,24,27] Among well-known trajectories, only the ρ can contribute, but none of the differential cross sections show the expected dip at $t = -0.5$ GeV^2.[28] Furthermore, the density matrix elements consistently disagree with ρ exchange dominance: pure ρ exchange implies $\rho_{00} = 0$, but the measured values average to one-half; and a reasonable model of the ρ-nucleon-isobar vertex[29,30] predicts Δ density matrix elements which also disagree with the data.[31]

This behavior is at least plausible in the light of the above kinematic separation. The ρ exchange is suppressed at the lowest t by kinematics and at $t = -0.5$ GeV^2 by a zero in the amplitude. It is not surprising, therefore, that it should be entirely masked by background effects, such as the possible exchange of a B meson ($\alpha_B \gtrsim \alpha_\rho - 1$).[32] If these are the only causes of suppression, the ρ trajectory contribution should rise above the background at large t and s. This would probably produce a small bump in the differential cross section above $t = -0.5$ GeV^2.

A further indication that spin suppression factors play a major role is provided by comparing the cross section for $\pi^+N^+ \to \omega N^{*++}$ with that for $\pi^+N^+ \to \pi^o N^{*++}$ at the same energy. Both reactions are expected to be dominated by ρ exchange, but whereas $\pi^+N^+ \to \pi^o N^{*++}$ differential cross sections consistently show a forward peak and a dip at $\alpha_\rho = 0$,[23,24] the $\pi^+N^+ \to \omega N^{*++}$ distribution in t is flat as

mentioned above. Plots of cos θ_t versus t for the two reactions show that the region over which spin suppression might affect $\pi p \to \pi N^*$ is considerably smaller ($|t| \leq 0.05$ GeV^2) than the comparable region for $\pi N \to \omega N^*$, and that much of the ρ peak for $\pi p \to \pi N^*$ falls within the "suppressed" region for ω production.

The shapes of the density matrix elements near t = 0 are also strongly influenced by the suppression factors. In the coordinate system in which these are normally measured,[33] the density matrix elements can be expressed entirely in terms of t-channel helicity amplitudes, $\rho_{ij} = \Sigma_\lambda T^i_\lambda T^j_\lambda / \Sigma_{k,\lambda} |T^k_\lambda|^2$ (i, j refer to the helicity of the particle under consideration, λ runs over all sets of other helicities in the problem). Unless a particular model is used, the behavior of the ρ_{ij} as a function of t is quite complex. However, the behavior for the lowest possible t is easily found (Table III.2).

These general results replace, in a Regge pole model, the expectations for pure π or vector meson exchange obtained from field theory. The elements ρ_{1-1}, ρ_{31}, and ρ_{3-1} are predicted to have a definite shape near the lowest t regardless of the parity exchanged; this shape can be seen most clearly in K^* production.[34,22] Additional assumptions must be made to obtain values for the constants which multiply these low t shapes, or to find the shapes at larger t.[35]

It is interesting to note that the suggested shapes strongly resemble the behavior near t = 0 of density matrices obtained on

Table III.2

Behavior as $t \to t_{min}$ of density matrix elements. Each expression may be multiplied by an arbitrary constant

$\pi B \to VB$

Parity of Exchanged Trajectory	ρ_{00}	ρ_{10}	ρ_{1-1}
$(-1)^{J+1}$	1	$\left\lvert \frac{\sin\theta_t}{s} \right\rvert$	$\left\lvert \frac{\sin^2\theta_t}{s^2} \right\rvert$
$(-1)^{J}$	0	0	$\lvert \sin^2\theta_t \rvert$

$\pi B \to V\Delta$

	ρ_{00}	ρ_{10}	ρ_{1-1}	ρ_{33}	ρ_{31}	ρ_{3-1}
$(-1)^{J+1}$	1	$\left\lvert \frac{\sin\theta_t}{s\sqrt{t}} \right\rvert$	$\left\lvert \frac{\sin^2\theta_t}{ts^2} \right\rvert$	$\frac{1}{s^2}$	$\left\lvert \frac{\sin\theta_t}{\sqrt{t}\,s} \right\rvert$	$\left\lvert \frac{\sin^2\theta_t}{ts^2} \right\rvert$
$(-1)^{J}$	0	0	$\left\lvert \frac{\sin^2\theta_t}{t} \right\rvert$	1	$\left\lvert \frac{\sin\theta_t}{\sqrt{t}} \right\rvert$	$\left\lvert \frac{\sin^2\theta_t}{t} \right\rvert$

the basis of the absorption model.[36] This behavior agrees with the bulk of data to date. The agreement of shape at low t between experiment and the two theories should thus not be viewed as a triumph of a particular dynamical model, but simply as an indication that the kinematical constraints have been handled properly in both theories. Until recently, it was not clear how to incorporate these into a Regge pole model. Hence the agreement in the density matrices provides a great deal of support for the methods of References 1 and 3.

The spin suppression effect is also expected to occur in tensor meson production. Because 2^+ mesons have natural parity, the helicity 0 state (and hence any M = 0 amplitudes) can be populated only by unnatural parity exchange. As in vector meson production, unnatural parity exchanges should thus dominate others in the forward peak.

Although relatively little data are available on the production of tensor mesons, the work of the British-German collaboration at 4 GeV/c provides some indications that spin suppression effects may explain features of these processes also. Consider, for example, the reactions $\pi^- p \to f_o n$, and $\pi^+ p \to A_2 p$. In $\pi^- p \to f_o n$, the π and A_2 exchanges are allowed. These are the same contributions expected in $\pi^- p \to \rho_o n$; it is found experimentally that the cross sections for the two reactions have sharp forward peaks indicating π dominance.[37] In contrast, the A_2 production differential cross section is relatively flat, resembling that for ω production.[23] A_2 production is like ω

production in that the only well-accepted trajectories which can contribute (ρ and f_o to $\pi N \rightarrow A_2 N$; ρ to $\pi N \rightarrow \omega N$) have natural parity.

Discussion

A. Careful treatment of kinematic effects and the use of daughter trajectories are only two elements of a complete Regge pole model of these reactions. There is no reason for them to completely determine the relative importance of various exchanges, particularly at lower energies. Other well-known explanations of pi dominance in such reactions as $\pi N \rightarrow \rho N$ include: (a) nearness of the pi pole to the s-channel physical region in t, and (b) the relatively large strength of couplings at the vertices. These facts certainly play an important role. The kinematic effect described here is quite distinct, however, and is by no means confined to pi exchange.

B. It is extremely difficult to obtain purely theoretical estimates of the magnitudes of Regge pole couplings. Some of the couplings can be obtained at the particle pole by comparison with Feynman graphs, but their variation with t cannot at present be predicted. For those couplings which vanish at the particle pole, there is no known way to theoretically estimate magnitudes at any t.

Because of the difficulty, it is felt that a least squares fitting program would be premature. In particular, it is essentially impossible to compare (for example) the magnitude of ρ and B exchange in ω production processes. Until such a comparison can be made, one cannot be certain how much of the suppression of natural parity exchange is due to the spin suppression effect discussed in this section.

Within the present Regge formalism, however, the $(\sin \theta_t/2)^{|\lambda-\mu|}(\cos \theta_t/2)^{|\lambda+\mu|} s^{\alpha-M}$ dependence will continue to play an important role.

3.2 Reggeization of Pi Exchange in Production Processes

It has been found[38,39] that in production reactions where π dominance is suspected, rapid variation of γ with t is required to fit the data at $t < 0$ and the known pole strength at $t = m_\pi^2$. In this section a study is made of reggeization of the pion, including both the Wang prescription for kinematic singularities and further kinematic relations at the $N\bar{\Delta}$ pseudothreshold. It is found that the rapid variation of $\gamma(t)$ is caused by these further kinematic effects, rather than by dynamics. These considerations suggest a model for $\gamma(t)$, which is then applied to several processes. The agreement with experiment is comparable to that obtained in the one pion exchange model with absorptive corrections.

Threshold Behavior

The factors provided by Wang were obtained, we recall, by a rather abstract crossing argument (Eqs. II.18 and II.19). As noted in Section 3.1, they can be checked by less abstract arguments based on the threshold behavior of partial-wave helicity amplitudes with definite parity. Since the threshold argument increases one's confidence and will be used extensively in the following sections, it is appropriate to work out an example showing how it goes at pseudothresholds as well as thresholds.

The example will be $\pi N \to \rho\Delta$, or rather the t-channel reaction $N\bar{\Delta} \to \rho\pi$. We take the amplitude $(f^t_{0\ 0;\frac{1}{2}\frac{1}{2}} + f^t_{0\ 0;-\frac{1}{2}\ -\frac{1}{2}})$ which is purely $P = (-1)^{J+1}$ and is therefore contributed to by $N\bar{\Delta} \to \pi \to \rho\pi$. The Wang prescription for this amplitude is

$$f^t_{0\ 0;\frac{1}{2}\ \frac{1}{2}} + f^t_{0\ 0;-\frac{1}{2}\ -\frac{1}{2}} = K^+_{0\ 0;\frac{1}{2}\ \frac{1}{2}}(t)\ \ \tilde{f}^t_{0\ 0;\frac{1}{2}\ \frac{1}{2}}(s,t) \quad , \qquad \text{(III.4)}$$

where[2)]

$$K^+_{0\ 0;\frac{1}{2}\ \frac{1}{2}}(t) = \frac{1}{[t-(m_\Delta+m_N)^2]\sqrt{(t-(m_\Delta-m_N)^2)\ (t-(m_\rho+m_\pi)^2)(t-(m_\rho-m_\pi)^2)}} \ . \qquad \text{(III.5)}$$

Now, what factors in

$$\bar{f}^t_{cd;ab} = \sum_J (2J+1)\ F^J_{cd;ab}(t)\ P^{(|\lambda-\mu|,\ |\lambda+\mu|}_{J-M}(\cos\theta_t) \qquad \text{(III.5)}$$

could explain these fixed singularities in t?

(i) At a <u>threshold</u>, $F^J(t)$ contains the usual factor $q_{in}^{\ell_{in}}\ q_{out}^{\ell_{out}}$ where

$$q_{in} = \frac{\sqrt{(t-(m_\Delta+m_N)^2)\ (t-(m_\Delta-m_N)^2)}}{2\sqrt{t}} \ , \qquad \text{(III.6)}$$

$$q_{out} = \frac{\sqrt{(t-(m_\rho+m_\pi)^2)\ (t-(m_\rho-m_\pi)^2)}}{2\sqrt{t}} \ . \qquad \text{(III.7)}$$

(ii) P_{J-M} is a polynomial in

$$\cos\theta_t = \frac{2\ s\ t + t^2 - t\ \Sigma\ m_i^2 + (m_\Delta^2 - m_N^2)\ (m_\rho^2 - m_\pi^2)}{4\ t\ q_{in}\ q_{out}} \ . \qquad \text{(III.8)}$$

The combination of these factors may give $\bar{f}^t$ an overall singularity or zero at either of the two thresholds $t = (m_\Delta + m_N)^2$ and $t = (m_\rho + m_\pi)^2$.

To see how to obtain the overall singularity at $t = (m_\Delta + m_N)^2$, consider $\ell_{in} = 0$. For this orbital state, the $N\bar{\Delta}$ system has $J^P = 1^-$ or 2^-. Since the particular amplitude we are considering has $P = (-1)^{J+1}$, the $N\bar{\Delta}$ system must have $J^P = 2^-$. For $\ell_{in} = 0$ there is no $q_{in}^{\ell_{in}}$ factor from F^J; for $J^P = 2^-$ (and with $M = 0$ for our particular example), $P_{J-M}^{(|\lambda-\mu|, |\lambda+\mu|)}(\cos\theta_t) = P_2^{(0,0)}(\cos\theta_t)$ is a second-order polynomial in $\cos\theta_t$ with leading singularity $q_{in}^{-2} \sim [t-(m_\Delta+m_N)^2]^{-1}$ (Eqs. (III.6) and (III.8)). This agrees with Wang's result, Eq. (III.5). For arbitrary ℓ_{in}, F^J picks up an additional factor $q^{\ell_{in}}$ but the most singular part of P_{J-M} picks up a compensating factor $q^{-\ell_{in}}$, so the overall singularity is unchanged. The key steps in this argument are tabulated in Table III.3, together with the corresponding steps which explain the factor at $t = (m_\rho + m_\pi)^2$.

Next we consider singularities at the <u>pseudothresholds</u>. It is helpful to think of the pseudothreshold $t = (m_\Delta - m_N)^2$ as a threshold involving the "antiparticle state," $E_N = -m_N$. Exactly the same arguments can be applied as above, except that the intrinsic parity of the "antiparticle state" is <u>reversed</u> relative to the particle state for a fermion (and <u>not reversed</u> for a boson). Thus, for $\ell_{in} = 0$, the "N"$\bar{\Delta}$ system has $J^P = 1^+$ or 2^+, and since the particular amplitude we are considering has $P = (-1)^{J+1}$, only $J^P = 1^+$

Table III.3

Threshold factors in the amplitude

$(\bar{f}^{t}_{0\ 0;\frac{1}{2}\ \frac{1}{2}} + \bar{f}^{t}_{0\ 0;-\frac{1}{2}\ -\frac{1}{2}})$ for $N\bar{\Delta} \to \rho\pi$.

Threshold	Lowest ℓ	Possible J^P for Lowest ℓ	Allowed J^P with $P = (-1)^{J+1}$	Threshold Factor
$t = (m_\Delta + m_N)^2$	$\ell_{in} = 0$	$1^-,\ 2^-$	2^-	$[t-(m_\Delta+m_N)^2]^{-1}$
$t = (m_\rho + m_\pi)^2$	$\ell_{out} = 0$	1^+	1^+	$[t-(m_\rho+m_\pi)^2]^{-\frac{1}{2}}$
$t = (m_\rho - m_\pi)^2$	$\ell_{out} = 0$	1^+	1^+	$[t-(m_\rho-m_\pi)^2]^{-\frac{1}{2}}$
$t = (m_\Delta - m_N)^2$	$\ell_{in} = 0$	$1^+,\ 2^+$	1^+	$[t-(m_\Delta-m_N)^2]^{-\frac{1}{2}}$

contributes. For $\ell_{in} = 0$ and $J = 1$, F^J gives no $q_{in}^{\ell_{in}}$ factor and P_{J-M} gives $q_{in}^{-1} \sim (t-(m_\Delta-m_N)^2)^{-\frac{1}{2}}$ which agrees with Wang's result, Equation (III.5). Again, the argument is summarized in Table III.3, together with the corresponding argument at $t = (m_\rho-m_\pi)^2$. Note that because of the parity change for fermions, the singularities are of different order at $t = (m_\Delta + m_N)^2$ and $t = (m_\Delta-m_N)^2$, whereas they are of the same order at $t = (m_\rho+m_\pi)^2$ and $t = (m_\rho-m_\pi)^2$.

The type of argument sketched above agrees with Wang's prescription in all cases checked.[40] At this time, no corresponding physical argument for the behavior at $t = 0$ is known.

The additional kinematic zeros described by Fox,[10] Cohen-Tannoudji et al.,[4] and others can also be interpreted in terms of threshold effects[41] (except for the relations at $t = 0$). We have already mentioned how this works out for $NN \to NN$ (see Ref. 14). In meson production reactions, the corresponding relations are quite complicated, but simplifications occur in the special case of pure $J^P = 0^-$ exchange which is relevant to the study of pion exchange.

For example, at $t = (M_\Delta - M_N)^2$ in $\pi N \to V\Delta$, the method of Cohen-Tannoudji et al.,[4] yields one condition connecting the $\lambda = 0$, $\mu = 0$ amplitude to other helicity amplitudes, and other conditions not involving $\lambda = 0$, $\mu = 0$. In the special case of pure $J^P = 0^-$ exchange, the first condition simplifies to $f_{\mu=0,\lambda=0}(t= (M_\Delta-M_N)^2) = 0$. The physical reason for the simplification is that a spin zero exchange couples exclusively to the $\lambda = 0$, $\mu = 0$ amplitude, so that the threshold conditions can only provide the $\lambda = 0$, $\mu = 0$ amplitude

with extra zeros in this case rather than relating it to other amplitudes. Similar behavior occurs at the other pseudothresholds and thresholds.

Elementary pion exchange is a familiar case in which the extra zeros of pure 0^- exchange appear. It is represented by a Feynman diagram which automatically satisfies all the kinematic relations. The amplitude for elementary pion exchange in $\pi N \to \rho\Delta$ has the form

$$f^t_{0\ 0;\ \frac{1}{2}\ \frac{1}{2}} + f^t_{0\ 0;-\frac{1}{2}\ -\frac{1}{2}} = \frac{K^+(t)\ \gamma_{e\ell}(t)}{t-m_\pi^2} \qquad \text{(III.9)}$$

where $K^+(t)$ has been given in Equation (III.5). Evaluation of the Feynman diagram gives

$$\gamma_{e\ell}(t) = c\ [t-(m_\Delta+m_N)^2]^2\ [t-(m_\Delta-m_N)^2]\ [t-(m_\rho+m_\pi)^2]\ [t-(m_\rho-m_\pi)^2] \qquad \text{(III.10)}$$

with the constant fixed by the known strength at the pole. The extra zeros provided by the workings of the kinematic relations for 0^- exchange are evident in (III.10).

To understand from an angular momentum point of view why the kinematic factors in 0^- exchange, as exemplified by elementary pion exchange, differ from the Wang K^+, we observe that the kinematic factor K^+ can be obtained by setting $\ell = 0$ and finding the corresponding J^P, whereas to obtain the elementary pion amplitude one must set $J^P = 0^-$ and find the corresponding ℓ. For example, at

$t = (m_\Delta + m_N)^2$ the intrinsic spin-parity of $N\bar{\Delta}$ is 1^- or 2^-, so to reach total $J^P = 0^-$ requires an orbital state $\ell_{in} = 2$. Then in the $J^P = 0^-$ contribution to f^t, $F^{J=0} \sim q_{in}^{\ 2}$ and $P_{J-M} = P_0 = \text{constant}$, so $f^t = (K^- \gamma_{el}/t-m_\pi^{\ 2}) \sim q_{in}^{\ 2} \sim [t-(m_\Delta+m_N)^2]$. This implies that γ_{el} picks up a factor $[t-(m_\Delta+m_N)^2]^2$, in agreement with Equation (III.10). A resume of the analogous arguments at the other thresholds is given in Table III.4.

Repeating the same arguments for, say, an elementary 2^- particle, one sees that it would <u>not</u> have a rapidly varying $\gamma(t)$ in the $\lambda = 0$, $\mu = 0$ amplitude. The reason in the present language is that it can couple to $N\bar{\Delta}$ or $\pi\rho$ in both $\ell > J$ and $\ell < J$ states, and the contribution to $\gamma(t)$ from the <u>lowest</u> ℓ does not vanish at threshold. Equivalently, one can say that a 2^- particle couples to several helicity amplitudes, and satisfies the threshold conditions by relations among these amplitudes rather than zeros in the $\lambda = 0$, $\mu = 0$ amplitude. The same is true for any particle on the sequence 1^+, 2^-, 3^+, ...[42] The rapid variation of $\gamma_{el}(t)$ for the pion, then, is a special feature of $J^P = 0^-$, which can couple only to $\lambda = 0$, $\mu = 0$, and $\ell > J$, and therefore has extra threshold zeros in the $\lambda = 0$, $\mu = 0$ amplitude.

<u>Models for $\pi N \to \rho\Delta$</u>

In this section we consider in succession three different models for pion exchange in $\pi N \to \rho\Delta$. The experimental density matrices for $\pi N \to \rho\Delta$ in the forward peak indicate that the non-helicity change amplitude with $\mu = 0 = \lambda$ dominates.[43] It therefore

Table III.4

Threshold factors in the elementary pion exchange contribution to the amplitude $(f^t_{0\ 0;\frac{1}{2}\ \frac{1}{2}} + f^t_{0\ 0;-\frac{1}{2}\ -\frac{1}{2}})$ for $N\bar{\Delta} \to \rho\pi$.

Threshold	J^P	Intrinsic Spin and Parity	ℓ Needed To Make J^P	Factor for K γ_π	Factor for γ_π Alone
$t = (m_\Delta+m_N)^2$	0^-	$1^-,2^-$	$\ell_{in} = 2$	$[t-(m_\Delta+m_N)^2]$	$[t-(m_\Delta+m_N)^2]^2$
$t = (m_\rho+m_\pi)^2$	0^-	1^+	$\ell_{out} = 1$	$\sqrt{t-(m_\rho+m_\pi)^2}$	$(t-(m_\rho+m_\pi)^2)$
$t = (m_\rho-m_\pi)^2$	0^-	1^+	$\ell_{out} = 1$	$\sqrt{t-(m_\rho-m_\pi)^2}$	$(t-(m_\rho-m_\pi)^2)$
$t = (m_\Delta-m_N)^2$	0^-	$1^+,2^+$	$\ell_{in} = 1$	$\sqrt{t-(m_\Delta-m_N)^2}$	$(t-(m_\Delta-m_N)^2)$

makes sense to focus our attention on this amplitude, which is the one dissected in the previous section.

Of the two possible $\mu = 0 = \lambda$ amplitudes $(f^t_{0\ 0;\frac{1}{2}\ \frac{1}{2}} \pm f^t_{0\ 0;-\frac{1}{2}\ -\frac{1}{2}})$, the - combination vanishes on account of parity conservation. The + combination (Eq. (III.4)) is purely $P = (-1)^{J+1}$. Writing the Regge representation for $\tilde{f}^t_{0\ 0;\frac{1}{2}\ \frac{1}{2}}$, approximating it by the pion trajectory, and keeping only the leading power at large s, one obtains

$$\left(f^t_{0\ 0;\frac{1}{2}\ \frac{1}{2}} + f^t_{0\ 0;-\frac{1}{2}\ -\frac{1}{2}} \right) \xrightarrow[s \to \infty]{}$$

$$K^+_{0\ 0;\frac{1}{2}\ \frac{1}{2}}(t)\ \gamma_\pi(t) \left(\frac{s}{s_o}\right)^{\alpha_\pi(t)} \frac{\left(1+e^{-i\pi\alpha_\pi(t)}\right)}{\sin \pi\, \alpha_\pi(t)} \frac{\Gamma(\alpha_\pi+\frac{1}{2})\ (2\alpha_\pi+1)}{\Gamma(\alpha_\pi+1)} \tag{III.11}$$

where K^+ was given in Equation (III.5) and γ is the reduced residue function.

The first model is a straight line trajectory with constant dynamical coupling factor:

$$\alpha_\pi(t) = -0.02 + \frac{t}{(\text{GeV})^2} \quad , \tag{III.12}$$

$$\gamma_\pi(t) = \text{constant} \quad . \tag{III.13}$$

The constant is determined from the known strength of the pole at $t = m_\pi^2$, and s_o is chosen as $s_o = 2\sqrt{m_\pi m_\rho m_N m_\Delta} = 0.74\ (\text{GeV})^2$ (similar

results would be obtained with the commonly assigned value $s_o = 1(\text{GeV})^2$). The resulting forward peak (Fig. III.1b, curve (iii)) is much too sharp, falling far below the experimental cross section. The predicted cross section remains too low for models with flatter trajectories, as long as γ_π is held constant.

The second model is elementary pion exchange, as calculated from the Feynman diagram. The amplitude for this model, and the coupling $\gamma_{el}(t)$, have already been given in Equations (III.9) and (III.10). As t goes negative, $\gamma_{el}(t)$ is a rapidly rising function, which more than offsets K(t) and produces much too large a cross section (Fig. III.1a, curve (i)). The t-dependence of γ_{el} is crucial here; even if we revert to the straight line α_π with slope $1(\text{GeV})^{-2}$, the cross section remains too large as long as we retain $\gamma_{el}(t)$ (Fig. III.1a, curve (ii)).

One way of viewing the failure of elementary pion exchange is in terms of unitarity in the s-channel. The elementary pion exchange term does not include the influence of other channels, and even exceeds the unitarity bound in some low partial waves, so absorptive corrections must be made. This approach has been used in the report of the Aachen-Berlin-CERN collaboration;[24] it produces theoretical results quite near the data (Fig. III.1c, curve (vii)). The reggeized pion exchange of our first model, however, lies well below the data, so it is certainly below the unitarity bound. Some approach other than absorptive corrections is needed to improve the Regge model.

Another way of viewing the failure of these first two models is in terms of the t-channel threshold effects discussed at the end of the previous section. The first model ignores these effects completely. The second model, on the other hand, incorporates the special effects of $J^P = 0^-$ exchange even at thresholds where the Regge α is far from 0. These faulty approximations contrast with what is presumably the actual situation:

(i) The π trajectory couples mainly to the $\lambda = 0$, $\mu = 0$ amplitude, with the special threshold behavior of the elementary pion, at a pseudothreshold or threshold where $\alpha_\pi(t)$ is near enough to zero so that most of the contribution comes from the $J^P = 0^-$ state.

(ii) When α_π is far from zero, the trajectory couples to various helicity amplitudes, and the threshold conditions are satisfied by relations among helicity amplitudes rather than by zeros in the $\lambda = 0$, $\mu = 0$ amplitude.

The third and final model attempts to incorporate kinematic effects into the $\lambda = 0$, $\mu = 0$ amplitude more realistically, by taking $\gamma(t)$ variable but using the extra zeros of elementary pion exchange only at pseudothresholds and thresholds where α_π is near zero. For simplicity we again confine our attention to the $\lambda = 0$, $\mu = 0$ amplitude. This, of course, restricts the validity of the model to small t (say, $|t| \lesssim 0.2$ GeV^2), but that is the region where π exchange is most prominent anyway.

We again take the straight line approximation $\alpha_\pi(t) = -0.02 + t/(\text{GeV})^2$. The locations of the thresholds and

pseudothresholds for $N\bar{\Delta} \to \rho\pi$, and the corresponding values of α_π, are listed in Table III.5. At $t = (m_\Delta - m_N)^2$, α_π is only 0.07 and the Regge amplitude projects heavily onto the 0^- partial wave. Thus the Regge amplitude has a 0^- part (probably dominant) which vanishes at $t = (m_\Delta - m_N)^2$, and another part (the projection onto other partial waves, probably rather small) which does not vanish. It is plausible to represent the net effect by a (t-b) contribution to γ_{Regge}, where b is somewhat shifted from $(m_\Delta - m_N)^2$. At $t = (m_\rho + m_\pi)^2$ and $(m_\Delta + m_N)^2$, α_π is large, the projection onto higher partial waves whose coupling does not vanish at threshold is probably large, and there is no compelling reason to introduce another zero into γ_{Regge}. The point $t = (m_\rho - m_\pi)^2$ is intermediate and it is less clear what to do here.

These considerations lead to the approximate form $\gamma_{Regge} = c(t-b)$ where b is small, and c is determined from the known strength at $t = m_\pi^2$. The cross sections computed in this way with $b = 0.09\ (GeV)^2$ and with $b = -0.005\ (GeV)^2$ are compared with experiment[23,24] in Figures III.1b and III.1c. The fit with $b = (m_\Delta - m_N)^2 = 0.09(GeV)^2$ (curve (v)) already represents a great improvement over the simple Regge model with constant γ (curve (iii)). For smaller b, the fit becomes comparable to that obtained with absorptive corrections to elementary pion exchange (Fig. III.1c). By taking $b < m_\pi^2$, the "hook" in the experimental cross section is also obtained (curves (iv) and (vi)), although $b < m_\pi^2$ admittedly departs from the spirit in which the model was derived.

Although this "hook" appears regularly in experimental data presented for $\pi B \to V\Delta$, there is a possibility that it is spurious --

Table III.5

Location of thresholds and pseudothresholds of $N\bar{\Delta} \to \pi\rho$, and corresponding values of $\alpha_\pi(t) = -0.02 + t/(\text{BeV})^2$.

Threshold	t in $(\text{BeV})^2$	α_π
$t = (m_\Delta - m_N)^2$	0.09	0.07
$t = (m_\rho - m_\pi)^2$	0.37	0.35
$t = (m_\rho + m_\pi)^2$	0.79	0.77
$t = (m_\Delta + m_N)^2$	4.75	4.73

an effect caused not by nature but by the method of analysis chosen. This is because for large t, all Δ and V events within a mass band of width ~ 100 MeV are counted in determining the cross section. For very small t, the heavier Δ's and V's will not be counted

$$(\text{as } t_{min} = - \frac{(m_\nu^2 - m_\pi^2)\ (m_\Delta^2 - m_N^2)}{s} + 0\left(\frac{1}{s^2}\right)$$

will be larger than some reported t for these large mass values); hence the cross section will appear to decrease. If this be the case, the "hook" should disappear when the differential cross sections are plotted against angle.[44] Until this experimental question is resolved, it should be borne in mind that fits to $d\sigma/dt$ can be made with b on either side of m_π^2 .

Comparison of the Model with Other Reactions

The purpose of this section is to show that the model of pion residue functions developed for $\pi N \to \rho\Delta$ above also fits the differential cross sections for $\pi N \to \rho N$, $KN \to K^*\Delta$, $\pi N \to f^0\Delta$, and $\pi N \to f^0 N$ at small t.

First, some comments which apply both to $\pi N \to \rho\Delta$ and to the reactions considered in the present section:

(i) A complete study of residue functions would involve a great deal more than comparison of differential cross sections. One would first separate the contributions of different helicity amplitudes to the cross section on the basis of density matrix elements and s and t dependence. Then individual residue functions for various exchanges could be isolated and studied. Some work along these lines has been done by Thews.[38] The purpose of this section, however, is only to

indicate dominant features of the situation and such a detailed study has not been undertaken.

(ii) For all reactions considered here, the density matrix elements and s-dependence at small t are compatible with the assumption that pion exchange in the $\lambda = 0$, $\mu = 0$ amplitudes dominates. The graphs below show that the t-dependence of $d\sigma/dt$ can also be understood on the basis of this assumption. The comparison with data must be confined to small t, however, because the assumption is expected to fail at $|t| \gtrsim 0.2$ $(GeV)^2$ on both theoretical and experimental grounds. Experiments[25,45] on the density matrices of produced ρ's, for example, show that for $|t| \gtrsim 0.2$ $(GeV)^2$ a large percentage of the vector mesons produced are transversely polarized, which implies $\mu \neq 0$. Thus the model developed above for the $\lambda = 0$, $\mu = 0$ amplitude will be judged successful if it approximately fits $d\sigma/dt$ for $|t| \lesssim 0.2$ $(GeV)^2$ and tends to fall below the data for $|t| \gtrsim 0.2$ $(GeV)^2$, leaving room for other amplitudes.

(iii) To specify the model somewhat more fully than was done above, let us discuss the various terms in some detail. Under the assumption that $f_{\lambda=0,\mu=0}(\pi \text{ exchange})$ (Eq. (III.11)) dominates the forward peak, the differential cross section can be written as

$$\frac{d\sigma}{dt} = \frac{1}{4\pi\,[s-(m_1+m_2)^2]\,[s-(m_1-m_2)^2]} \left| K(t)\, \gamma_\pi(t) \left(\frac{s}{s_o}\right)^{\alpha_\pi(t)} \frac{\left(1+e^{-i\pi\alpha_\pi}\right)}{\sin \pi\alpha_\pi} \frac{\Gamma(\alpha_\pi+\frac{1}{2})\ (2\alpha_\pi+1)}{\Gamma(\alpha_\pi+1)} \right|^2 \qquad \text{(III.14)}$$

where m_1 and m_2 are the masses of the incident pseudoscalar and baryon for the reaction under consideration. The factor $\Gamma(\alpha_\pi+\frac{1}{2})/\Gamma(\alpha_\pi+1)$ is a coefficient of s^{α_π} in the asymptotic expansion of $P_\alpha(\cos\theta_t)$; the variations of these Γ functions and $(2\alpha_\pi+1)$ over the small range of t considered is not extremely important. The kinematic factor $\bar{K}(t)$ for each reaction is taken from Wang[2,3] and listed in Table III.6; for reactions of type $\pi + N \to (\rho \text{ or } f^0) + N$ it includes the factor t which Wang derived[3] from the factorization condition (see Section 3.1). A straight line with slope 1 $(GeV)^{-2}$ has been used to approximate $\alpha_\pi(t)$. The reduced residue function $\gamma_\pi(t)$ suggested by considerations above has the form γ = constant (t-b) for the reactions involving an $N\bar{\Delta}$ vertex; a similar consideration of the reactions involving an $N\bar{N}$ vertex yields the form γ = constant, since in this case the nearby pseudothreshold has moved to $t = (m_N-m_{\bar{N}})^2 = 0$ and $\gamma_{el\ \pi}(t)$ has no zeros at t = 0. The value of each $\gamma_\pi(t)$ at $t = m_\pi^2$ is known from the experimental coupling strengths for $\rho\pi\pi$, $f^0\pi\pi$, $K^*K\pi$, $NN\pi$, and $\Delta N\pi$. These values are listed in Table III.6. The remaining parameter b has been treated as a variable, and we discuss below some of the values which give good fits. Finally, the scale factor s_o has been chosen as $2\sqrt{m_1m_2m_3m_4}$, which is not far from 1 GeV^2 for all cases considered. This choice is not crucial; fits with similar b's could be obtained for a wide range of s_o ($0.5\ GeV^2 \lesssim s_o \lesssim 5\ GeV^2$).

With this background, one can quickly determine the peculiarities of individual reactions.

Table III.6

The Wang kinematic factor $\bar{K}(t)$, and the strength of the dynamical residue function $\gamma_\pi(t)$ at $t = m_\pi^2$, for pion trajectory exchange in various reactions. The symbol τ_{ij} denotes $[(t-(m_i+m_j)^2)(t-(m_i-m_j)^2)]^{\frac{1}{2}}$

Reaction	$\bar{K}(t)$	$\gamma_\pi(t=m_\pi^2)/(\text{mb})^{\frac{1}{2}}$
$\pi^+ p \to \rho^o \Delta^{++}$	$\tau_{\rho\pi}^{-1}\ \tau_{N\Delta}^{-1}\ [\sqrt{t-(m_N+m_\Delta)^2}]^{-1}$	4.5 GeV^6
$\pi^- p \to \rho^o n$	$\sqrt{t}\ \tau_{\rho\pi}^{-1}$	9.9 GeV^2
$K^+ p \to K_o^* \Delta^{++}$	$\tau_{KK^*}^{-1}\ \tau_{N\Delta}^{-1}\ [\sqrt{t-(m_N+m_\Delta)^2}]^{-1}$	2.5 GeV^6
$\pi N \to f^o N$	$\sqrt{t}\ \tau_{\pi f}^{-2}$	67.2 GeV^4
$\pi^+ p \to f^o \Delta^{++}$	$\tau_{\pi f}^{-2}\ \tau_{N\Delta}^{-1}\ [\sqrt{t-(m_N+m_\Delta)^2}]^{-1}$	30.5 GeV^8

$\pi^+ p \to \rho^o \Delta^{++}$: The cross section for $b = (m_\Delta - m_N)^2 = 0.09$ GeV^2 is shown in Figures III.1b (curve (v)). The best fit, which gives the "hook" visible in the 8 GeV/c data in Figure 1c, as well as at lower energies,[43] is given by $b = -0.005$ GeV^2 (curves (iv) and (vi)).

$\pi^- p \to \rho^o n$: The cross section of form (III.14) with K and γ_π taken from Table III.6, fits the data [46] quite well (Fig. III.2) without additional parameters.

$K^+ p \to K_o^* \Delta^{++}$: The differential cross section for this reaction in the extreme forward direction is not well known at present. As a result, there are two solutions of the form indicated above which fit the data points[47] -- one solution with $b = 0.045$ GeV^2 and the other with $b = 0.001$ GeV^2. They are both plotted in Figure III.3.

$\pi N \to f^o N$: As in the analogous reaction $\pi N \to \rho^o N$, the cross section[48,49] can be fit quite well by use of a constant residue function with the kinematic factor and γ_π ($t = m_\pi^2$) of Table III.6 (Fig. III.4).

$\pi^+ p \to f^o \Delta^{++}$: Fitting this reaction with a linear residue function we find, as in the case of $\pi N \to \rho^o \Delta$, that the zero must fall at $t < 0$ ($b = -0.015$) in order to reproduce the "hook" at low t (Fig. III.5). Again a fit to the magnitude outside the hook region can be obtained with a zero at the $N\bar{\Delta}$ pseudothreshold.

Discussion

A. Mandelstam[50] has noticed a difficulty which arises in the formal reggeization of processes involving particles with higher spins. Normal methods of continuation in angular momentum produce, for

example, contributions to the Regge residues for $\pi N \to VN$ from $\ell = -1$ states. This is in contrast to the arguments above, in which only physical orbital angular momenta $\ell \geq 0$ to the t-channel have been considered. Mandelstam has also demonstrated,[50] however, that the contributions from unphysical ℓ may be cancelled by other terms, if all of the external particles involved lie on Regge trajectories. Thus the restriction to physical orbital angular momenta conforms to the result one presumably obtains by consistently reggeizing all hadrons both internal and external.

B. Dashen and Frautschi[29] have predicted from static model bootstrap calculations that

$$\frac{\beta_{\pi N\bar{N}}(t)}{\beta_{\pi N\bar{\Delta}}(t)} \approx \text{const} \quad . \tag{III.15}$$

This relation has been tested in various contexts[51,52] and found to be in agreement with vector meson production data. It is interesting to note that Equation III.15 would not be consistent with β's deduced purely from kinematic factors, but is roughly consistent at negative t with the behavior we have found from angular momentum considerations, $\beta_{\pi N\bar{\Delta}} \sim (t-B)\sqrt{t-(m_\Delta - m_N)^2}$.

C. Kinematic conditions affect the couplings of all trajectories. The existence and detection of the very rapid variation of $\gamma_\pi(t)$ in $\pi N \to \rho\Delta$, however, depends on the close conjunction of:

(a) the pole with large residue at $t = m_\pi^2$,

(b) the pseudothreshold with kinematic zero at $t = (m_\Delta - m_N)^2 =$

$0.09\ \text{GeV}^2$, and

(c) the physical region where the resulting residue variation can be observed at $t < 0$.

This close conjunction of all three effects is a unique feature of π exchange.

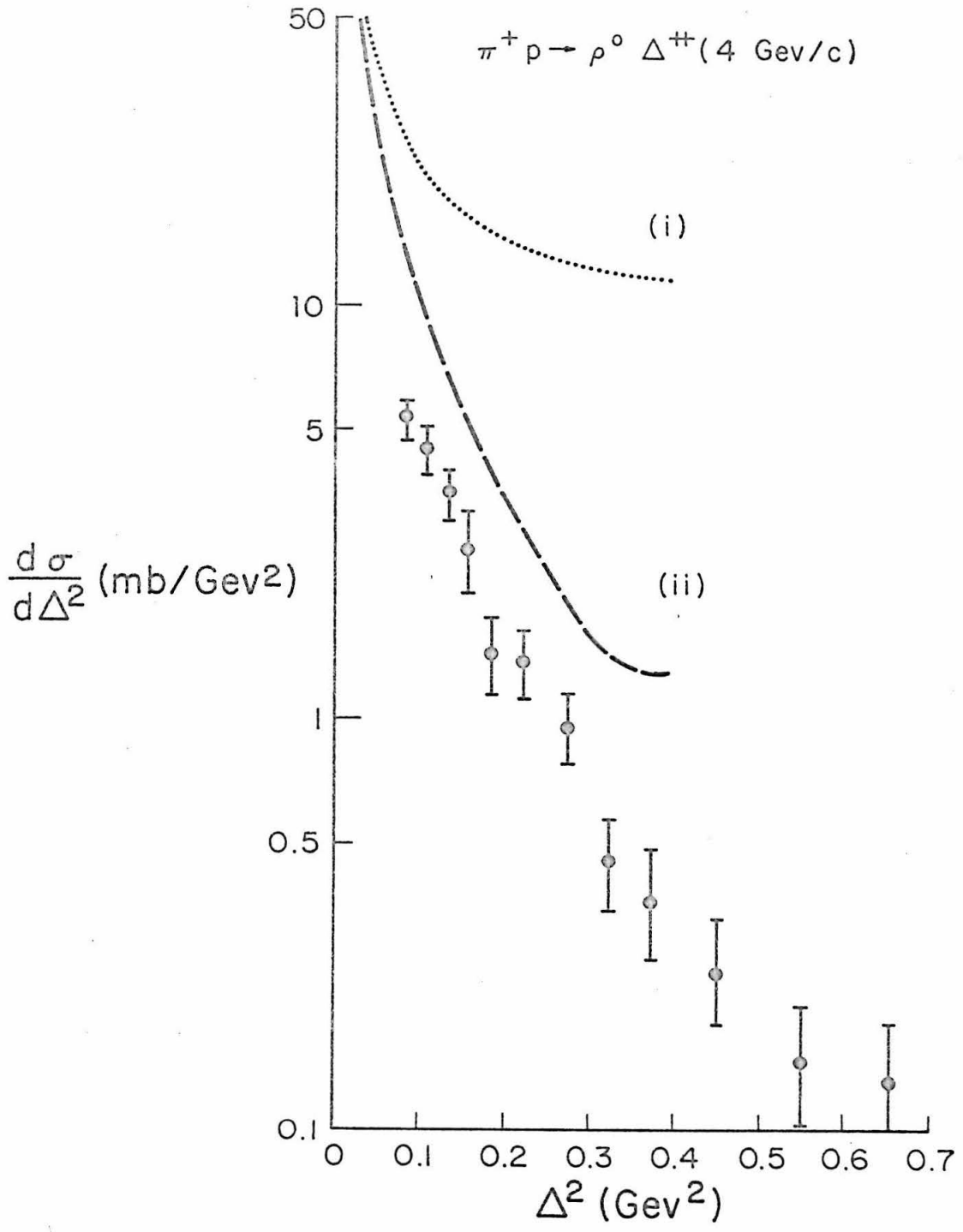

Figure III.1a

$\pi^+ p \rightarrow \rho^0 \Delta^{++}$ at 4 GeV/c. The data are from the British-German collaboration (Ref. 23). The curves represent: (i) elementary OPE; and (ii) reggeized OPE with kinematic factors of elementary exchange.

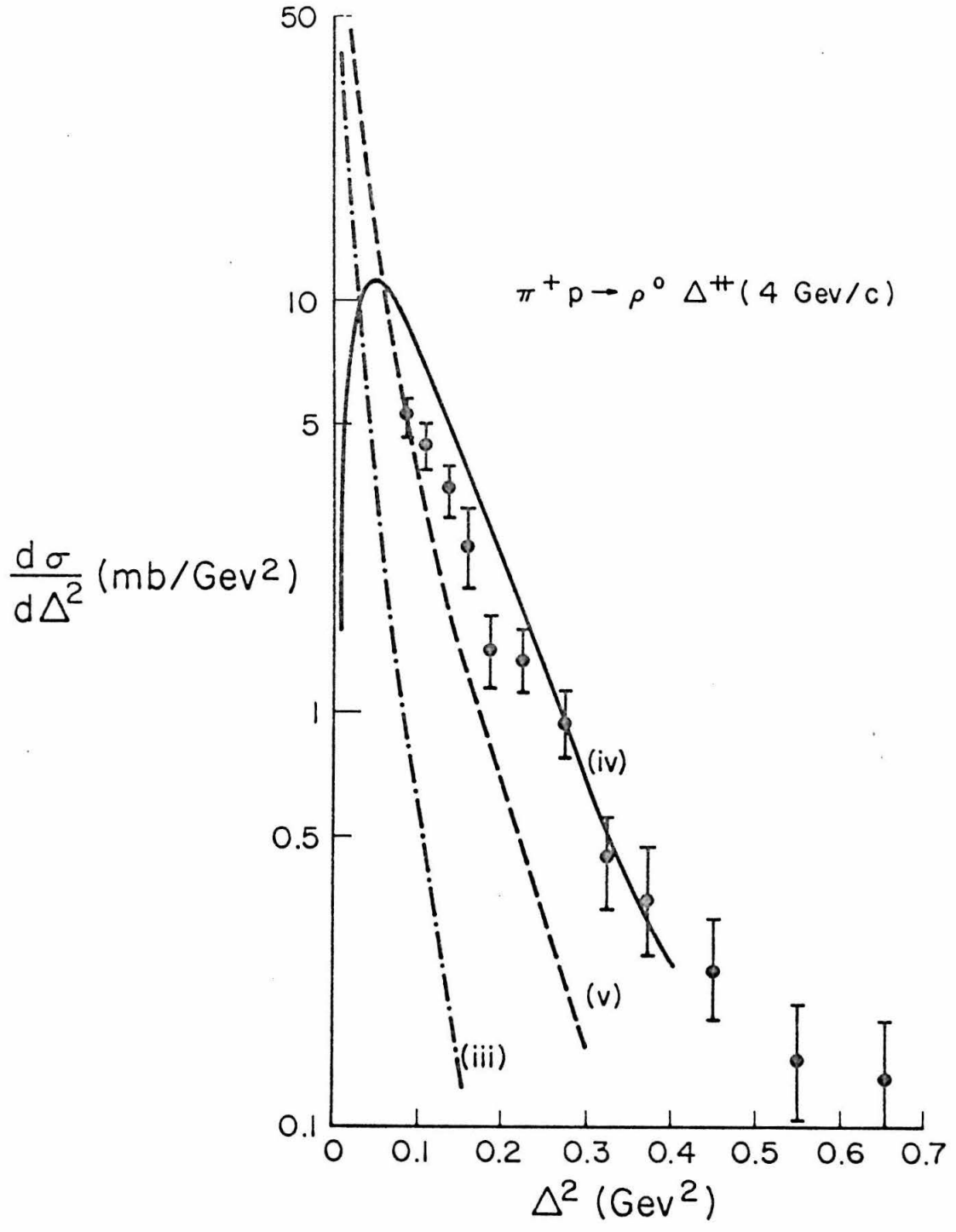

Figures III.1b

Comparison of the same data with: (iii) reggeized OPE with constant residue; kinematic factors from crossing matrix; (iv) reggeized OPE with linear residue (b = -0.005 GeV^2), kinematic factors from crossing matrix; (v) same model as (iv) with b = 0.09 GeV^2.

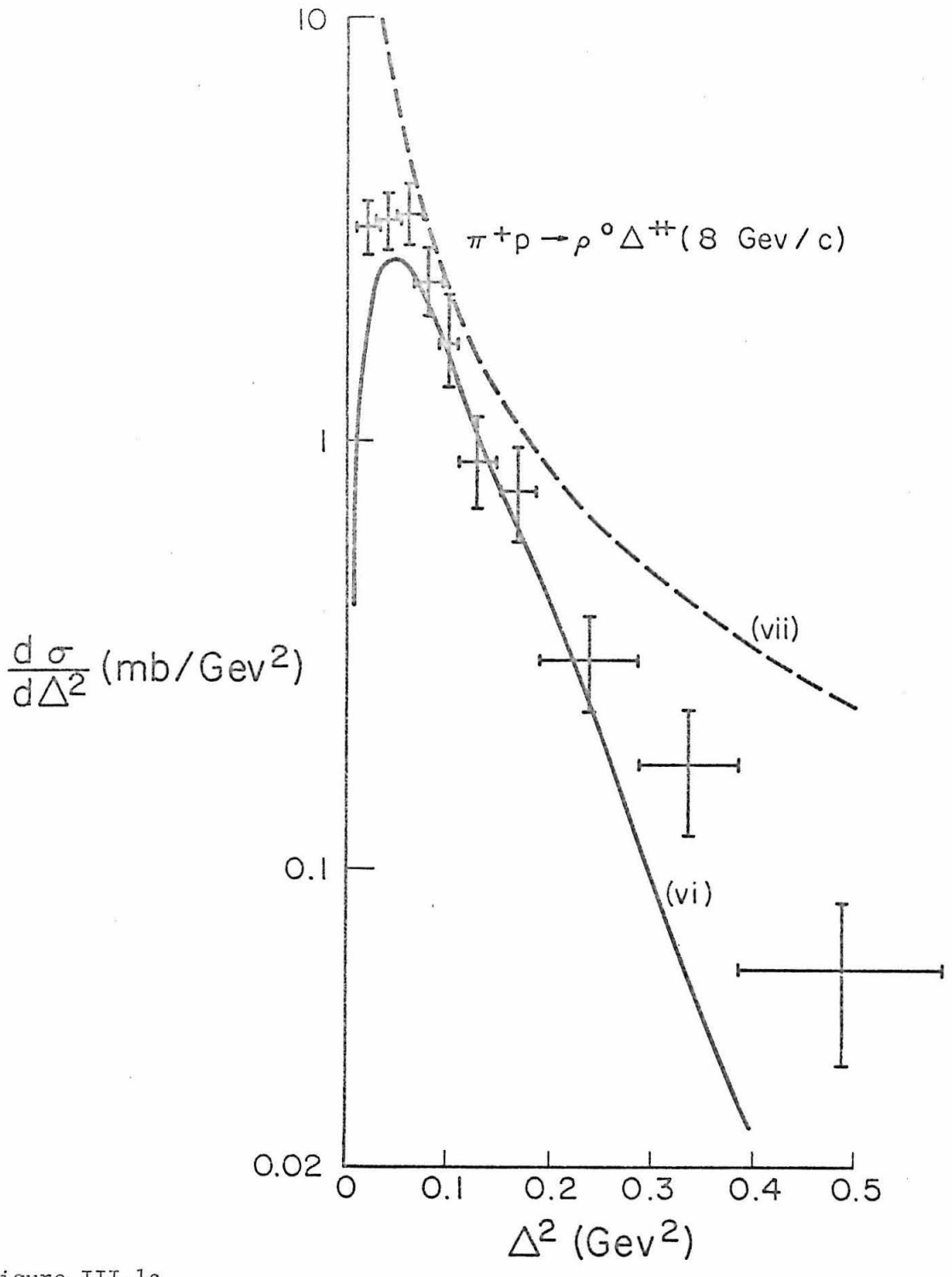

Figure III.1c

$\pi^+ p \to \rho^0 \Delta^{++}$ at 8 GeV/c. The data are from the Aachen-Berlin-CERN collaboration (Ref. 24). The curves represent: (vi) reggeized OPE with linear residue (b = -0.005 GeV^2), kinematic factors from crossing matrix; and (vii) absorbed OPE (calculation in Ref. 24).

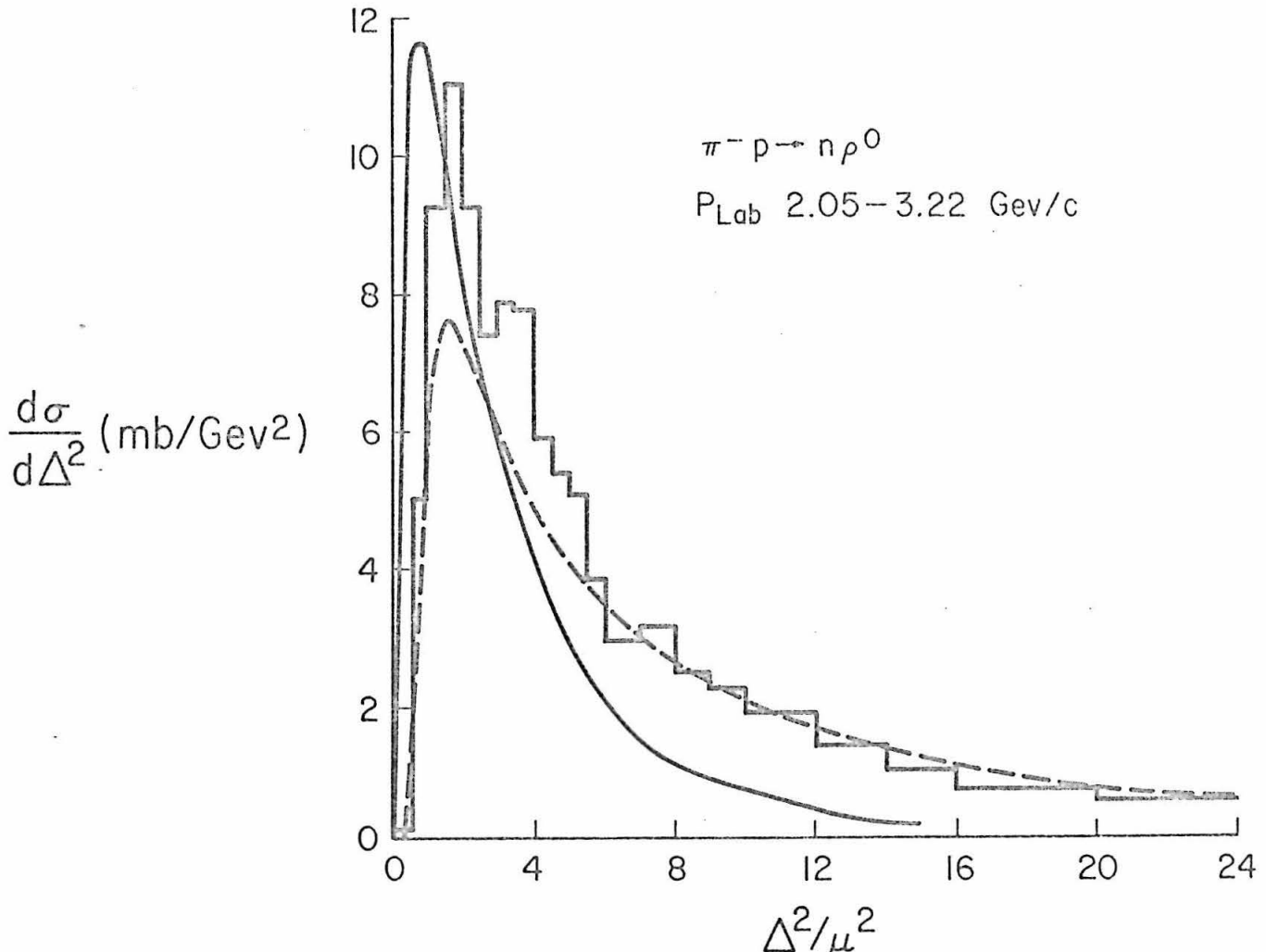

Figure III.2 $\pi^- p \to \rho^0 n$ at 2.05 - 3.22 GeV/c. The data are from Jacobs (Ref. 46). The broken line is absorbed OPE (calculation from Ref. 46). The solid line is reggeized OPE with kinematic factors from crossing matrix and factorization, constant residue.

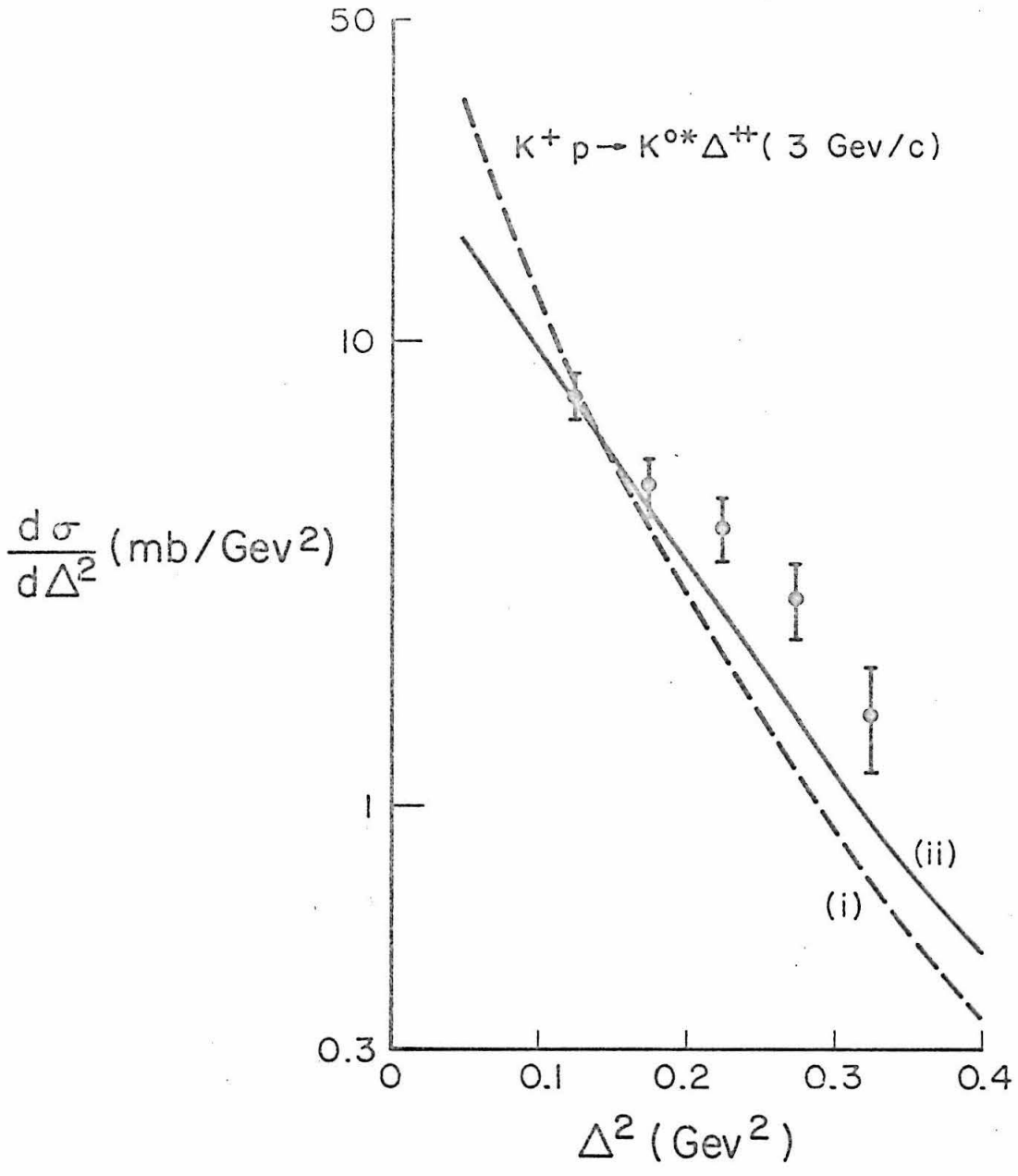

Figure III.3a

$K^+p \to K^{*o} \Delta^{++}$ at 3 GeV/c. The data are that of the CERN-Brussels collaboration (Ref. 47). The curves represent two possible fits with reggeized OPE, kinematic factors from crossing matrix, and linear residue function: The solid line corresponds to b = 0.001 GeV^2, the broken line to b = 0.045 GeV^2.

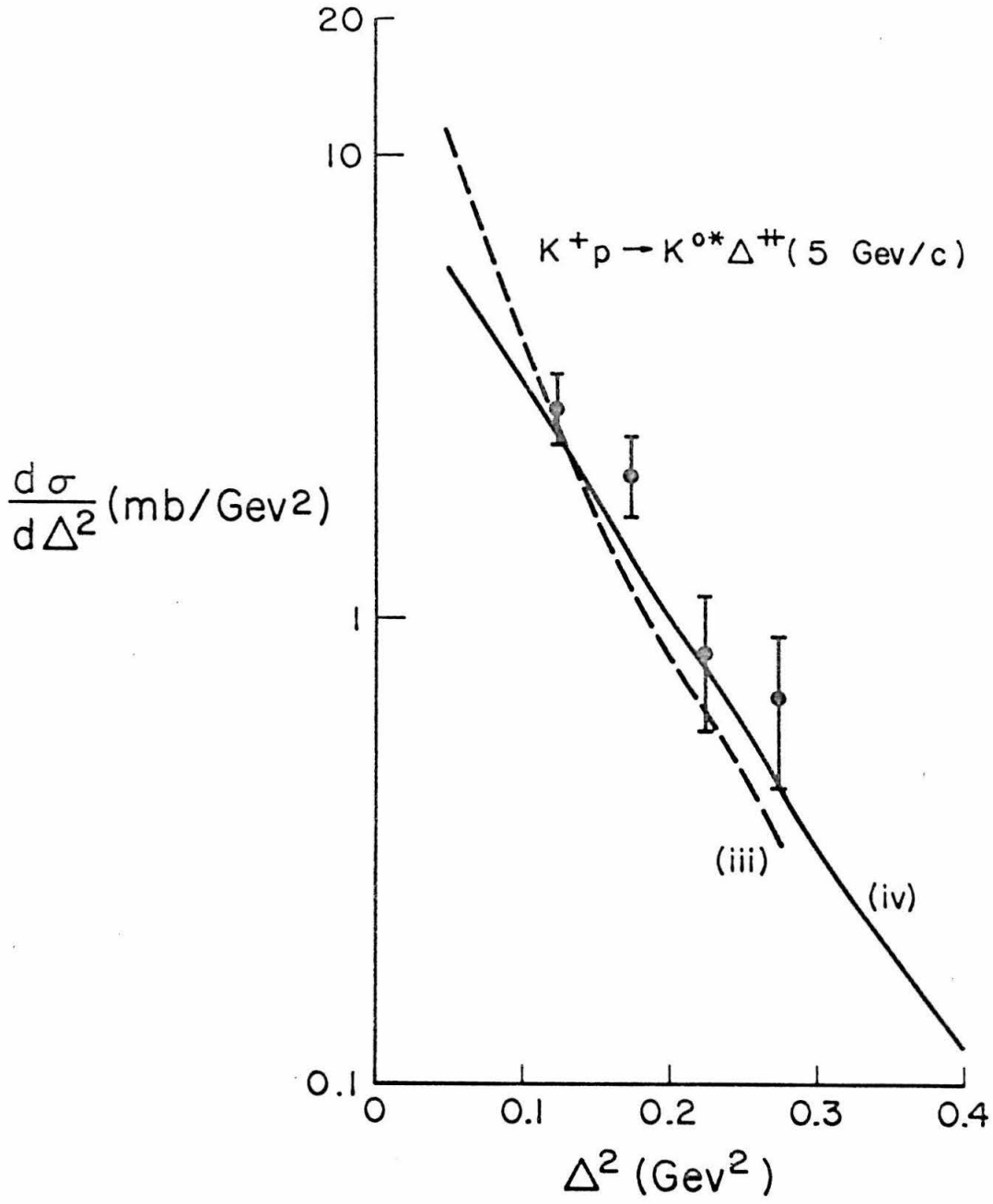

Figure III.3b

The same reaction and models as 3a, at 5 GeV/c.

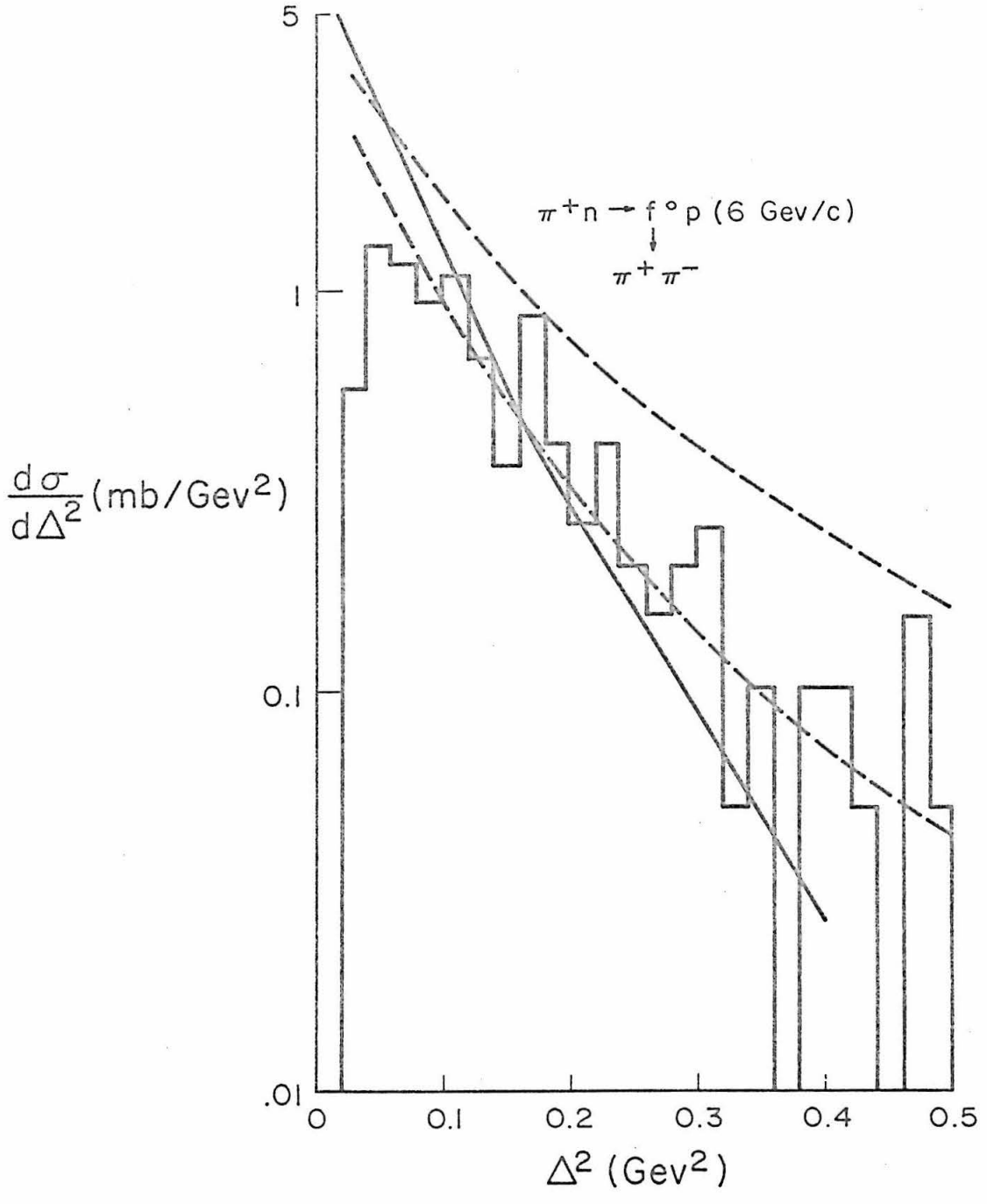

Figure III.4a

$\pi^+ n \rightarrow f^\circ p$ at 6 GeV/c. The data are from Bruyant et al. (Ref. 48). The broken lines are various absorption model predictions (calculations by Yock and Gordon (Ref. 39). The solid line represents reggeized OPE with kinematic factors from crossing matrix and factorization, constant residue.

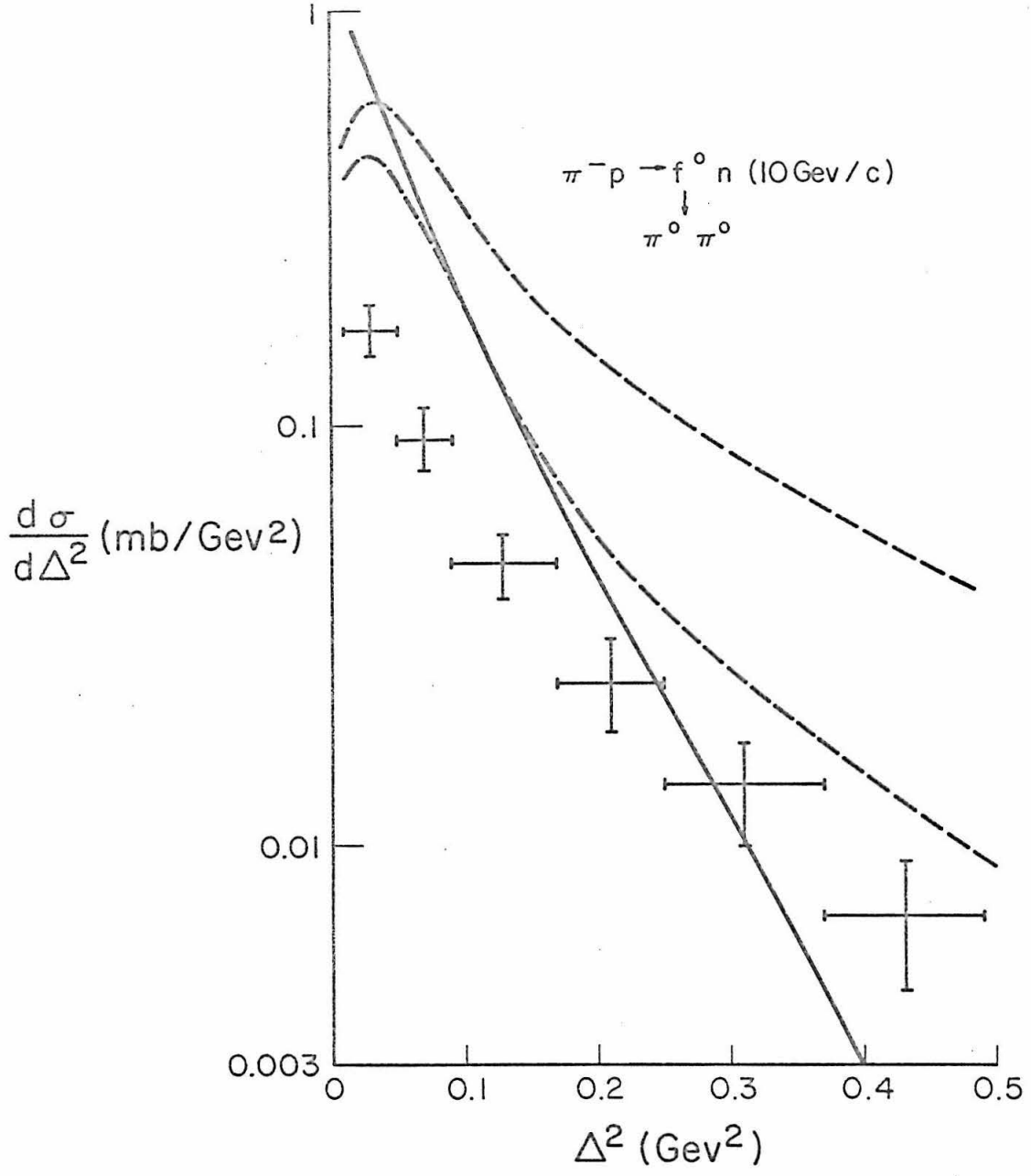

Figure III.4b

$\pi^- p \to f^0 n$ at 10 GeV/c. The data are from Wahlig et al. (Ref. 49). The curves have the same significance as in 4a.

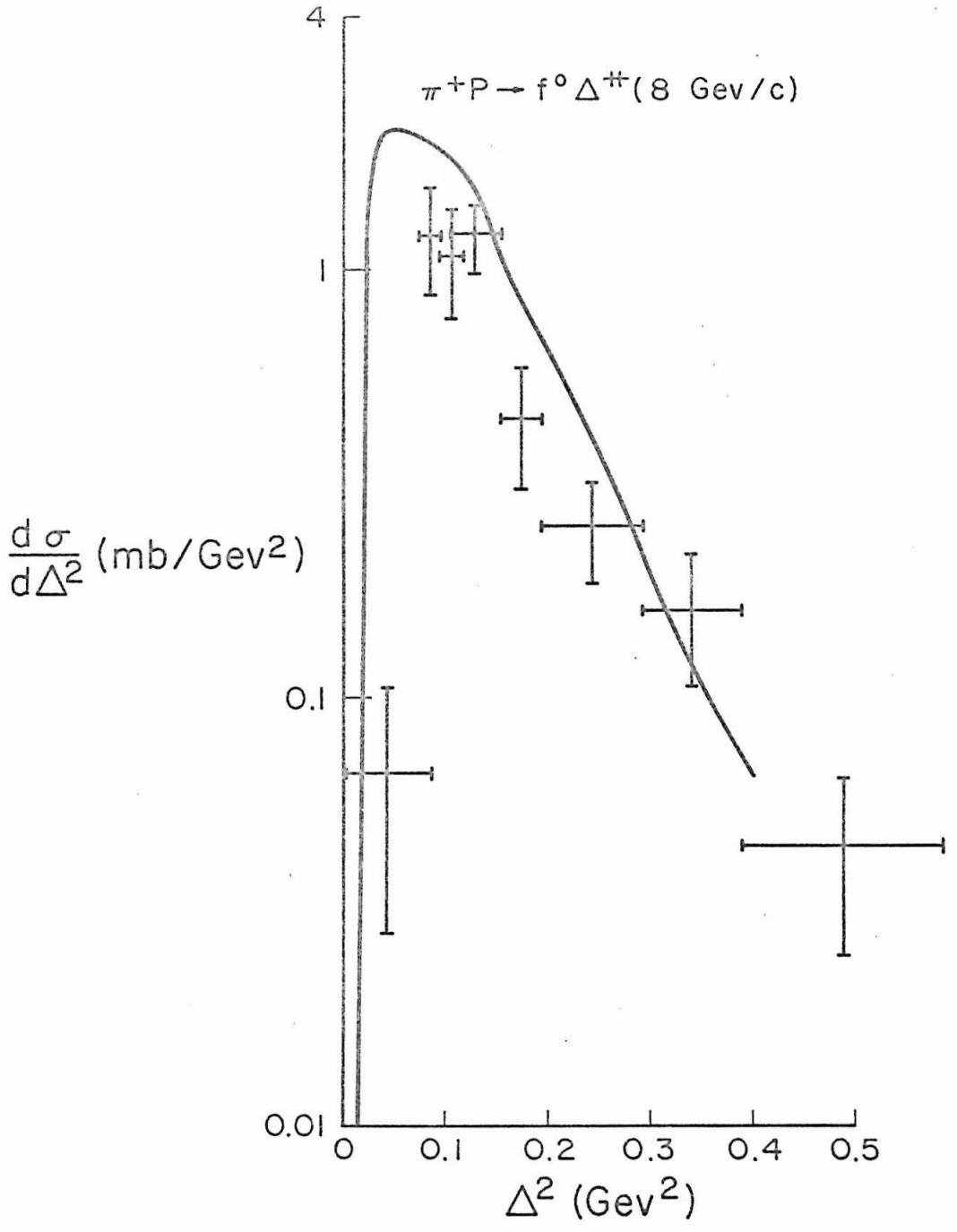

Figure III.5

$\pi^+ p \to f^\circ \Delta^{++}$ at 8 GeV/c. The data are from the Aachen-Berlin-CERN collaboration (Ref. 24). The curve represents reggeized OPE with kinematic factors from crossing matrix, linear residue (b=-0.015 GeV^2).

Chapter 4

ROLE OF CONSPIRACY IN THEORY OF VECTOR MESON PRODUCTION

Application of the methods of Chapter 2 yields two conspiracy relations at t = 0 for $\pi N \to VN$:[53]

$$\sqrt{t}\,(\bar{f}^{t}_{10;\frac{1}{2}-\frac{1}{2}} - \bar{f}^{t}_{-10;\frac{1}{2}-\frac{1}{2}}) = -i\sqrt{t}\,(f_{10;\frac{1}{2}\,\frac{1}{2}} - \bar{f}^{t}_{-10;\frac{1}{2}\,\frac{1}{2}}) \qquad \text{(IV.1)}$$

$$\sqrt{t}\;\bar{f}^{t}_{0\;0;\frac{1}{2}-\frac{1}{2}} = -2i\sqrt{t}\;f^{t}_{0\;0;\frac{1}{2}\,\frac{1}{2}} \qquad \text{(IV.2)}$$

For all four parity-conserving amplitudes involved here, the Wang kinematical factor K allows a $t^{-\frac{1}{2}}$ behavior at t = 0 (Table IV.1A). The additional kinematic conditions imposed by Equations (IV.1) and (IV.2) can be satisfied in either of two ways: a) each of the two amplitudes involved in an equation can have an additional factor of t from $\tilde{f}$; in this case each side of the equation would vanish separately like t (no conspiracy), or b) each amplitude can retain the singular $t^{-\frac{1}{2}}$ behavior at t = 0; in this case the two sides of the equation must approach the same constant (conspiracy). For example, one conspiracy solution behaves like

$$\begin{aligned} \bar{f}^{t}_{10;\frac{1}{2}\,\frac{1}{2}} - \bar{f}^{t}_{-10;\frac{1}{2}\,\frac{1}{2}} &= c_4\sqrt{t} \\ \bar{f}^{t}_{10;\frac{1}{2}-\frac{1}{2}} - \bar{f}^{t}_{-10;\frac{1}{2}-\frac{1}{2}} &= -i\,c_4\sqrt{t} \end{aligned} \qquad \text{(IV.3)}$$

near t = 0.

For the reaction $\pi N \to V\Delta$, the $t = 0$ conditions obtained by the methods of Chapter 2 (see Appendix A) are:

$$t^{3/2}\left[\bar{f}^{t}_{10;3/2-\frac{1}{2}} + \bar{f}^{t}_{-10;3/2-\frac{1}{2}}\right] = -t^{3/2}\left[\bar{f}^{t}_{10;3/2-\frac{1}{2}} - \bar{f}^{t}_{-10;3/2-\frac{1}{2}}\right] \qquad \text{(IV.4)}$$

$$t\left[\bar{f}^{t}_{10;\frac{1}{2}-\frac{1}{2}} + \bar{f}^{t}_{-10;\frac{1}{2}-\frac{1}{2}}\right] = -t\left[\bar{f}^{t}_{10;\frac{1}{2}-\frac{1}{2}} - \bar{f}^{t}_{-10;\frac{1}{2}-\frac{1}{2}}\right] \qquad \text{(IV.5)}$$

$$t\left[\bar{f}^{t}_{10;3/2\ \frac{1}{2}} + \bar{f}^{t}_{-10;3/2\ \frac{1}{2}}\right] = -t\left[\bar{f}^{t}_{10;3/2\ \frac{1}{2}} - \bar{f}^{t}_{-10;3/2\ \frac{1}{2}}\right] \qquad \text{(IV.6)}$$

In each of these amplitudes $\bar{f}^{t}_{cd;ab} \pm \bar{f}^{t}_{-c-d;ab}$ the Wang kinematic factor K (Table IV.1B) allows a maximum singularity $(\sqrt{t})^{-|c-d|-|a-b|}$ at $t = 0$ -- just enough to cancel the explicit factors of t in Equations (IV.4) and (IV.6). Again the $t = 0$ conditions can be satisfied either by having each side of the equation vanish separately like t, or by conspiracy between the coefficients of the singularities.

The discussion in Chapter 3 demonstrated that presently available data on vector meson production can be understood within the framework of the no-conspiracy (evasive) solutions. To obtain an understanding of the entire range of behavior allowed by kinematics, however, one must also examine the consequences of conspiracy. General properties of the conspiratorial solutions are discussed in this chapter; application to the particular case of photoproduction, where they appear to be needed, is made in Chapter 5.

Conspiracy and Angular Momentum Conservation in the Forward Direction

It has been known for some time that in NN scattering, the double spin flip amplitude $f^{s}_{\frac{1}{2}\frac{1}{2};-\frac{1}{2}-\frac{1}{2}}$ is non-zero in the forward direction only when conspiracy occurs, despite the fact that angular momentum conservation places no restrictions on this amplitude. The purpose of this section is to demonstrate that conspiracy has the same role in unequal mass reactions: that of restoring the contributions of double flip amplitudes to full strength in the forward direction.

As discussed in Chapter 2, although $\cos \theta_t/2$ and $\sin \theta_t/2$ are large and proportional to $s^{\frac{1}{2}}$ for larger t, they are constrained to approach 0 and 1 respectively at $\theta_s = 0^o$ ($t = t_{min}$). This means that all amplitudes

$$f^{t}_{co;ab} = \bar{f}^{t}_{co;ab} (\sin \theta_t/2)^{|c-a+b|} (\cos \theta_t/2)^{|c+a-b|} \qquad \text{(IV.7)}$$

with $(c+a-b) \neq 0$ vanish in the forward direction of the s-channel. For $(c+a-b) = 0$, the forward amplitude does not vanish but the fast drop in drop in $\sin \theta_t/2$ toward $t = t_{min}$ tends to suppress it. Unless $\bar{f}^{t}_{co;ab}$ for $(c+a-b) = 0$ compensates by growing like t^{-x} with appropriate x, the suppression will greatly decrease $f^{t}_{co;ab}$ near $t = t_{min}$.

It is instructive to view these same phenomena from the point of view of the s-channel amplitudes. As shown in Appendix B, at $\theta_s = 0^o$ the crossing relations reduce to the form

$$f^{t}_{co;ab} = \pm f^{s}_{-ca;ob} \quad . \tag{B.5}$$

The vanishing of all $f^{t}_{co;ab}$ with $c + a-b \neq 0$ at $\theta_s = 0^o$, then, is simply a manifestation of angular momentum conservation along the direction of forward scattering in the s-channel. The suppression of $f^{t}_{co;ab}$ with $(c+a-b) = 0$ at $\theta_s = 0^o$, however, is not required by angular momentum conservation. Therefore it is to be expected that $\bar{f}^{t}_{co;ab}$ can have the compensating factor t^{-x} needed to restore the normal size of the angular momentum conserving amplitudes at $\theta_s = 0^o$.

For reactions such as $\pi N \to V\Delta$, $\sin \theta_t/2 \sim \sqrt{ts}$ at high s; the forward suppression is caused by the $\sqrt{t}$ factor. Hence if $\bar{f}^{t}_{co;ab} \sim (1/\sqrt{t})^{|c-a+b|}$, we see from Equation (IV.7) that the amplitudes allowed by angular momentum conservation will contribute with full strength in the forward direction. This is exactly the maximum singularity allowed by the Wang formalism. As shown (Eqs. (IV.4) - (IV.6) and Table IV.1B), the amplitudes will have this maximum singularity only if they conspire at $t = 0$.

For $\pi N \to VN$, $\sin \theta_t/\pi \sim t^{\frac{1}{4}} s^{\frac{1}{2}}$ at high s; the forward suppression is caused by the $t^{\frac{1}{4}}$ factor. Hence, for this case, the $t = 0$ behavior necessary to ensure full contribution of the angular-momentum-conserving amplitude is $\bar{f}^{t}_{co;ab} \sim (t^{-\frac{1}{4}})^{|c-a+b|}$. Again we see from Table IV.1 that the relevant amplitude $\bar{f}^{t}_{-1\ 0;\frac{1}{2}\ -\frac{1}{2}}$, is allowed just the right singularity $(t^{-\frac{1}{4}})^{|c-a+b|} \sim t^{-\frac{1}{2}}$ in the Wang formalism, but (in view of Equation (IV.1) can achieve it only through conspiracy.

Hence we conclude that the conspiracy relations play a very similar role in equal and unequal mass reactions. In both cases non-conspiring flip-flip amplitudes vanish at t = 0; the main difference is that t = 0 corresponds exactly to forward scattering in the equal mass case, but is only approached asymptotically by forward production in the unequal mass case.

Conspiracy relation (IV.2) is in a separate category, since the $\lambda = \mu = 0$ amplitude is not multiplied by half angle factors and thus is not subject to quite the same suppression in the forward direction. In the no-conspiracy case, however, it does contain a $\sqrt{t}$, which along the curve $\theta_s = 0^o$ contributes an effective suppression $\sim s^{-1}$. In the case of conspiracy, Equation (IV.2) equates $f^t_{0\ 0;\frac{1}{2}\ \frac{1}{2}}$ to $(i/2)\ \bar{f}^t_{0\ 0;\frac{1}{2}\ -\frac{1}{2}}$, which grows like $s^{\alpha-1}\ t^{-\frac{1}{2}}$. Since $t^{-\frac{1}{2}} \sim s$ along the boundary curve, $f^t_{0\ 0;\frac{1}{2}\ \frac{1}{2}}$ will grow like s^{α} at $\theta_s = 0^o$, i.e., a conspiring singularity contributes full strength to the $\lambda = \mu = 0$ amplitude along the forward direction.

Table IV.1A

Amplitudes for $\pi N \to VN$

Amplitudes	μ	λ	Dominant Parity	Kinematic Factor	Extra Factor in No-Conspiracy Case
$f^t_{00;\frac{1}{2}\,\frac{1}{2}}$	0	0	$(-1)^{J+1}$	$1/\sqrt{t}$	t
$\bar{f}^t_{00;\frac{1}{2}\,-\frac{1}{2}}$	0	1	$(-1)^{J+1}$	$1/\sqrt{t}$	t
$\bar{f}^t_{10;\frac{1}{2}\,\frac{1}{2}} + \bar{f}^t_{-10;+\frac{1}{2}\,+\frac{1}{2}}$	1	0	$(-1)^{J}$	1	
$\bar{f}^t_{10;\frac{1}{2}\,\frac{1}{2}} - \bar{f}^t_{-10;+\frac{1}{2}\,+\frac{1}{2}}$	1	0	$(-1)^{J+1}$	$1/\sqrt{t}$	t
$\bar{f}^t_{10;\frac{1}{2}\,-\frac{1}{2}} + \bar{f}^t_{-10;+\frac{1}{2}\,-\frac{1}{2}}$	1	1	$(-1)^{J+1}$	1	
$\bar{f}^t_{10;\frac{1}{2}\,-\frac{1}{2}} - \bar{f}^t_{-10;+\frac{1}{2}\,-\frac{1}{2}}$	1	1	$(-1)^{J}$	$1/\sqrt{t}$	t

Table IV.1B

Amplitudes for $\pi N \to V\Delta$

Amplitudes	μ	λ	Dominant Parity	Kinematic Factor	Extra Factor in No-Conspiracy Case
$f^t_{00;\frac{1}{2}\,\frac{1}{2}}$	0	0	$(-1)^{J+1}$	1	
$\bar{f}^t_{00;3/2\,\frac{1}{2}}$	0	1	$(-1)^{J+1}$	$1/\sqrt{t}$	
$\bar{f}^t_{00;3/2\,-\frac{1}{2}}$	0	2	$(-1)^{J+1}$	$1/t$	
$\bar{f}^t_{00;\frac{1}{2}\,-\frac{1}{2}}$	0	1	$(-1)^{J+1}$	$1/\sqrt{t}$	
$\bar{f}^t_{10;\frac{1}{2}\,\frac{1}{2}} + \bar{f}^t_{-10;\frac{1}{2}\,\frac{1}{2}}$	1	0	$(-1)^{J}$	$1/\sqrt{t}$	
$\bar{f}^t_{10;\frac{1}{2}\,\frac{1}{2}} - \bar{f}^t_{-10;\frac{1}{2}\,\frac{1}{2}}$	1	0	$(-1)^{J+1}$	$1/\sqrt{t}$	
$\bar{f}^t_{10;\frac{1}{2}\,-\frac{1}{2}} + \bar{f}^t_{-10;\frac{1}{2}\,-\frac{1}{2}}$	1	1	$(-1)^{J+1}$	$1/t$	t
$\bar{f}^t_{10;\frac{1}{2}\,-\frac{1}{2}} - \bar{f}^t_{-10;\,\frac{1}{2}\,-\frac{1}{2}}$	1	1	$(-1)^{J}$	$1/t$	t
$\bar{f}^t_{10;3/2\,\frac{1}{2}} + \bar{f}^t_{-10;3/2\,\frac{1}{2}}$	1	1	$(-1)^{J+1}$	$1/t$	t
$\bar{f}^t_{10;3/2\,\frac{1}{2}} - \bar{f}^t_{-10;3/2\,\frac{1}{2}}$	1	1	$(-1)^{J}$	$1/t$	t
$\bar{f}^t_{10;3/2\,-\frac{1}{2}} + \bar{f}^t_{-10;3/2\,-\frac{1}{2}}$	1	2	$(-1)^{J+1}$	$1/t^{3/2}$	t
$\bar{f}^t_{10;3/2\,-\frac{1}{2}} - \bar{f}^t_{-10;3/2\,-\frac{1}{2}}$	1	2	$(-1)^{J}$	$1/t^{3/2}$	t

Chapter 5

CONSPIRACY IN THE REACTION $\gamma p \to \pi^+ n$

Because $\gamma p \to \pi^+ n$ is a special case of the class of reactions $\pi N \to VN$, time reversed, the forward dip displayed by Equation (II.12) and discussed in Section 3.1 should again apply to all amplitudes with $\mu \neq 0$ if there is no conspiracy. But photoproduction has the special feature that there <u>is</u> no amplitude with $\mu = h_\pi - h_\gamma = 0$; therefore, the dip should show up directly in the cross section and does not have to be disentangled from a dominant non-flip contribution in the usual fashion.

Due to this special feature, photoproduction is an especially favorable reaction for establishing whether conspiracy exists. At present, there are three strong indications that conspiracy does exist in photoproduction.

i) Halpern[54] has noted that the invariant amplitude conventionally labeled[55] A_1 vanishes at $t = 0$ unless there is conspiracy. But the low energy data, as discussed by Adler and Gilman[56] and by Halpern[54], indicate that A_1 does <u>not</u> vanish at $t = 0$.

ii) Evaluation of Feynman diagrams for the s-channel nucleon pole[57] leads to $A_1(t = 0) \neq 0$ at $s = M^2$. For this (s,t), no other diagram can cancel the pole; hence we can conclude that conspiracy is indeed present.

iii) Finally, there is the above point that the differential cross section would exhibit a forward dip were there no conspiracy.[58] The absence of a forward dip at low energies[59] agrees with the con-

clusion of i) and ii). Our t-channel analysis in terms of Regge poles is, however, more relevant to high energy data. At the highest energies measured, the differential cross section for $\gamma + p \to \pi^+ + n$ (Fig. V.1) appears to be rising as one approaches small angles,[59] strongly suggesting conspiracy. As explained below, measurements of the 0° cross section at high energy should settle the question definitively.

Kinematics of Photoproduction

The four independent combinations of helicity amplitudes needed to describe photoproduction, and the kinematic factor K for each of them, are listed in Table V.1. In evaluating K, there are special problems associated with the zero mass of the photon, and the K listed in Table V.1 is the limit as $m_V \to 0$ of K evaluated for the amplitudes with $m_V \neq 0$. The reasons why this choice has been made are given in Appendix C.

It is also straightforward to express the four invariant amplitudes A_i of Ball[55] in terms of the t-channel helicity amplitudes $\bar{f}^t$. This is done in Table V.2.

Now as $t \to 0$, let each helicity amplitude behave like the corresponding kinematic factor K(t) listed in Table V.1. The effect of this behavior of the A_i is easily deduced from Table V.2. One finds that all A_i can be non-zero at $t = 0$. A_2 will have a $1/t$ singularity, however, unless the coefficient of the $1/t$ term satisfies the condition

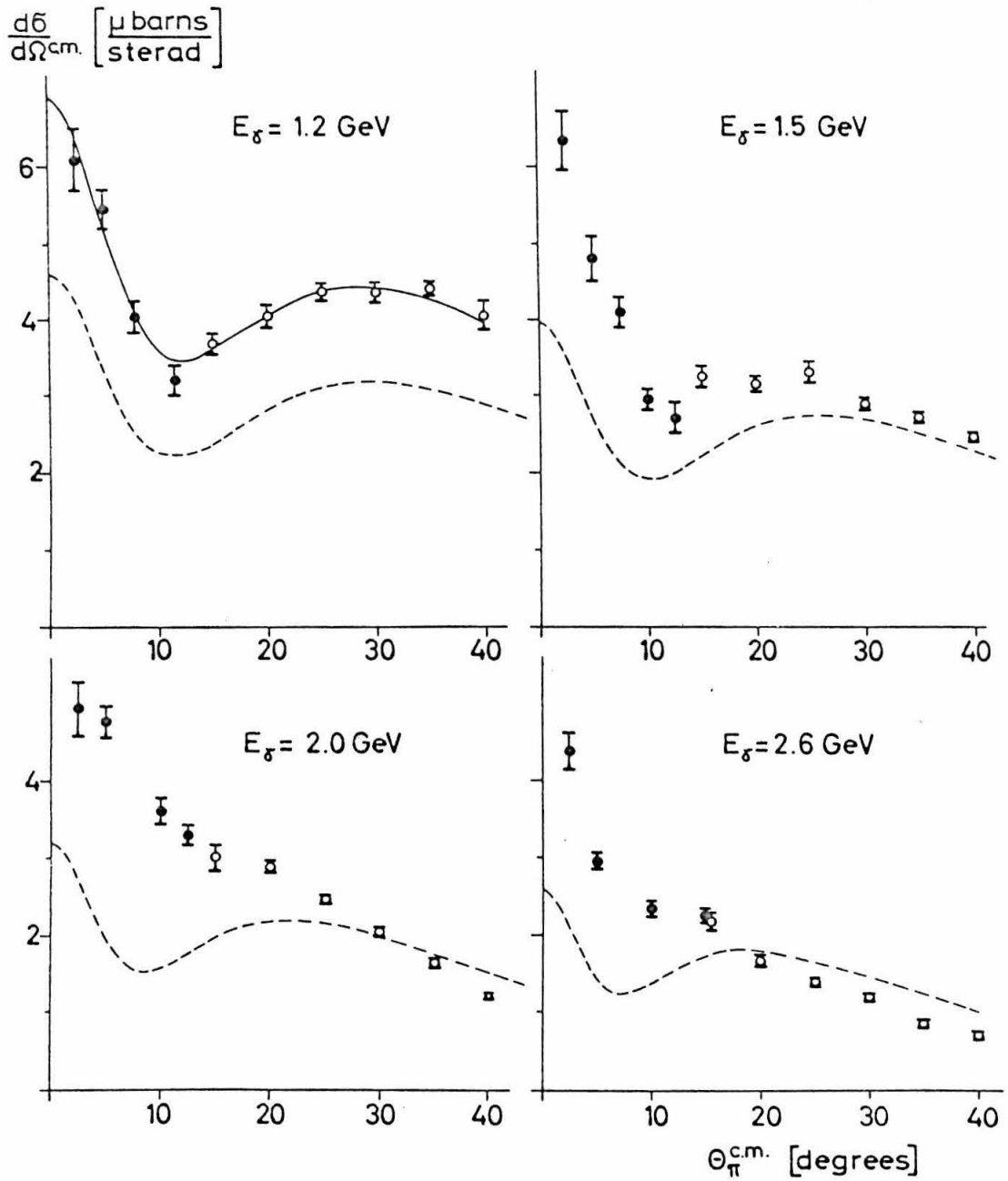

Figure V.1

Center-of-mass differential cross sections $d\sigma/d\Omega$ ($\gamma p \rightarrow \pi^+ n$) as a function of pion c.m. angle $\theta_\pi^{c.m.}$ for different incident photon energies E_γ, reproduced from Buschhorn et al. (Ref. 59). The broken lines may be disregarded.

$$(\bar{f}^t_{01;\frac{1}{2}\,\frac{1}{2}} - \bar{f}^t_{01;-\frac{1}{2}-\frac{1}{2}}) = -i\,(\bar{f}^t_{01;\frac{1}{2}\,-\frac{1}{2}} + \bar{f}^t_{01;-\frac{1}{2}\,\frac{1}{2}}) \qquad (V.1)$$

(this relation can also be found by the techniques of Section 2.2). Equation (V.1) can be satisfied in either of two ways:

i) By conspiracy among the different types of Regge trajectory (or cuts or fixed poles in angular momentum) involved in Equation (V.1). This has been studied by Halpern,[54] Mitter,[60] and Sawyer.[61]

ii) By individual vanishing ($\sim t$) of the Regge residues on the left and right-hand sides of Equation (V.1). The extra factors of t in this "no-conspiracy" solution are indicated by the * in Table V.1. Note that in this case, with $(\bar{f}^t_{01;\frac{1}{2}\,\frac{1}{2}} - \bar{f}^t_{01;-\frac{1}{2}\,-\frac{1}{2}})$ and $(\bar{f}^t_{01;\frac{1}{2}\,-\frac{1}{2}} + \bar{f}^t_{01;-\frac{1}{2}\,\frac{1}{2}})$ behaving like $t^{\frac{1}{2}}$ instead of $t^{-\frac{1}{2}}$, the amplitude A_1 in Table V.2 vanishes at $t = 0$. As stated above, this is the basis of Halpern's arguments for the existence of conspiracy in photoproduction.

The equations written thus far have referred to helicity amplitudes; this is all one needs to establish the properties of forward photoproduction discussed below. To express the conspiracy relations in terms of Regge trajectories, however, a partial wave expansion of the helicity amplitudes is necessary. In the form

$$\bar{f}^t_{cd,ab} = \sum_J (2J+1)\, T^J_{cd,ab}(t)\; P^{(|\lambda-\mu|,\,|\lambda+\mu|)}_{J-M}(\cos\theta_t)\,, \qquad (V.2)$$

partial wave amplitudes with definite parity are

Table V.1

Kinematic Singularities and Partial Wave Expansions of the Helicity Amplitudes for Photoproduction

Amplitude	$\lvert\lambda\rvert$	$\lvert\mu\rvert$	K(t)	Partial Wave Expansion	Dominant Parity
$\bar{f}^t_{01;\frac{1}{2}\,\frac{1}{2}} + \bar{f}^t_{01;-\frac{1}{2}\,-\frac{1}{2}}$	0	1	$(t-\mu^2)$	$\Sigma(2J+1)\, b_J^+ P^{(1,1)}_{J-1} \cos\theta_t)$	$(-1)^J$
$\bar{f}^t_{01;\frac{1}{2}\,\frac{1}{2}} - \bar{f}^t_{01;-\frac{1}{2}\,-\frac{1}{2}}$	0	1	$\frac{(t-4M^2)^{\frac{1}{2}}}{t^{\frac{1}{2}}}$ *	$\Sigma(2J+1)\, b_J^- P^{(1,1)}_{J-1} (\cos\theta_t)$	$(-1)^{J+1}$
$\bar{f}^t_{01;\frac{1}{2}\,-\frac{1}{2}} + \bar{f}^t_{01;-\frac{1}{2}\,\frac{1}{2}}$	1	1	$\frac{(t-\mu^2)}{t^{\frac{1}{2}}}$ *	$\Sigma(J+\frac{1}{2})\left[a_J^-(P^{(2,0)}_{J-1}-P^{(0,2)}_{J-1})+ a_J^+(P^{(2,0)}_{J-1}+ P^{(0,2)}_{J-1})\right]$	$(-1)^J$
$\bar{f}^t_{01;\,\frac{1}{2}\,-\frac{1}{2}} - \bar{f}^t_{01;-\frac{1}{2}\,\frac{1}{2}}$	1	1	$(t-4M^2)^{\frac{1}{2}}$	$\Sigma(J+\frac{1}{2})\left[a_J^+(P^{(2,0)}_{J-1}-P^{(0,2)}_{J-1})+ a_J^-(P^{(2,0)}_{J-1}+ P^{(0,2)}_{J-1})\right]$	$(-1)^{J+1}$

*In the absence of conspiracy, these amplitudes should be multiplied by an extra factor t.

Table V.2

Relation Between Invariant Amplitudes A_i
and t-Channel Helicity Amplitudes

$$A_1 = \frac{2\sqrt{2}\,M}{(4M^2-t)(t-\mu^2)}\left[t\left(\bar{f}^t_{01;\frac{1}{2}\,\frac{1}{2}} + \bar{f}^t_{01;-\frac{1}{2}\,-\frac{1}{2}} \right) - 2M\sqrt{t}\left(\bar{f}^t_{01;\frac{1}{2}\,-\frac{1}{2}} + \bar{f}^t_{01;-\frac{1}{2}\,\frac{1}{2}} \right)\right]$$

$$A_2 = \frac{2\sqrt{2}\,M}{(t-4M^2)(t-\mu^2)}\left[\left(\bar{f}^t_{01;\frac{1}{2}\,\frac{1}{2}} + \bar{f}^t_{01;-\frac{1}{2}\,-\frac{1}{2}} \right) + \frac{\sqrt{t-4M^2}}{\sqrt{t}}\left(\bar{f}^t_{01;\frac{1}{2}\,\frac{1}{2}} - \bar{f}^t_{01;-\frac{1}{2}\,-\frac{1}{2}} \right) - \frac{2M}{\sqrt{t}}\left(\bar{f}^t_{01;\frac{1}{2}\,-\frac{1}{2}} + \bar{f}^t_{01;\,-\frac{1}{2}\,\frac{1}{2}} \right)\right]$$

$$A_3 = \frac{\sqrt{2}\,M}{\sqrt{t-4M^2}\,(t-\mu^2)}\left[\bar{f}^t_{01;\frac{1}{2}\,-\frac{1}{2}} - \bar{f}^t_{01;-\frac{1}{2}\,\frac{1}{2}} \right]$$

$$A_4 = \frac{2\sqrt{2}\,M}{(4M^2-t)(t-\mu^2)}\left[2M\left(\bar{f}^t_{10;\frac{1}{2}\,\frac{1}{2}} + \bar{f}^t_{01;-\frac{1}{2}\,-\frac{1}{2}} \right) - \sqrt{t}\left(\bar{f}^t_{01;\frac{1}{2}\,-\frac{1}{2}} + \bar{f}^t_{01;-\frac{1}{2}\,\frac{1}{2}} \right)\right]$$

$$a_J^{\pm} \equiv T^J_{01;\ \frac{1}{2}\ -\frac{1}{2}} \pm T^J_{01;\ -\frac{1}{2}\ \frac{1}{2}} \ , \tag{V.3}$$

$$b_J^{\pm} \equiv T^J_{01;\ \frac{1}{2}\ \frac{1}{2}} \pm T^J_{01;-\frac{1}{2}\ -\frac{1}{2}} \ . \tag{V.4}$$

Here, amplitudes with + superscriprts have $P = (-1)^J$, and amplitudes with - superscripts have $P = (-1)^{J+1}$, so that a_J^+ and b_J^+ refer to $N\bar{N}$ in the $^3J\pm1_J$ state, a_J^- to the ^3J_J state, and b^-_J to the ^1J_J state. The first two combinations of amplitudes $\bar{f}^t$ in Table V.1,

$$\bar{f}^t_{01;\frac{1}{2}\ \frac{1}{2}} \pm \bar{f}^t_{01;-\frac{1}{2}\ -\frac{1}{2}} = \sum_J (2J+1) \left(T^J_{01;\frac{1}{2}\ \frac{1}{2}} \pm T^J_{01;-\frac{1}{2}\ -\frac{1}{2}} \right) P^{(1,1)}_{J-1} \ , \tag{V.5}$$

are then easily expressed in terms of the b's, while the last two combinations in Table V.1,

$$\bar{f}^t_{01;\frac{1}{2}\ -\frac{1}{2}} \pm \bar{f}^t_{01;-\frac{1}{2}\ \frac{1}{2}} = \sum_J (2J+1) \left\{ T^J_{01;\frac{1}{2}\ -\frac{1}{2}} P^{(0,2)}_{J-1} \pm T^J_{01;-\frac{1}{2}\ \frac{1}{2}} P^{(2,0)}_{J-1} \right\} \ , \tag{V.6}$$

can be expressed in terms of the a's. The results are listed in Table V.1. Finally, by inserting the appropriate partial wave expansions in Equation (V.1) we obtain

$$\sum (2J+1)\ b_J^-\ P^{(1,1)}_{J-1}\ (\cos\theta_t) = -i\sum (J+\tfrac{1}{2}) \left[a_J^- \left(P^{(2,0)}_{J-1} - P^{(0,2)}_{J-1}\right) + a_J^+ \left(P^{(2,0)}_{J-1} + P^{(0,2)}_{J-1}\right) \right] \ . \tag{V.7}$$

This is the familiar form of the conspiracy relation, from which one can deduce ratios of the residues of the various conspiring trajectories.

Consequences of Conspiracy for the Photoproduction Cross Section

The differential cross section for photoproduction by unpolarized initial beams can be written

$$\frac{d\sigma}{d\Omega} = \frac{p_f}{16\pi^2 s p_i} \sum_{abcd} \left| f^t_{cd,ab} \right|^2 \qquad (V.8)$$

where Ω, p_i, and p_f represent the solid angle, initial momentum, and final momentum, all in the center of mass. Using the relations between $f^t_{cd,ab}$ and $f^t_{-c-d,-a-b}$ provided by parity conservation to reduce the number of amplitudes, we can rewrite (V.8) as

$$\frac{d\sigma}{d\Omega} = \frac{p_f}{16\pi^2 s p_i} \left\{ \begin{array}{l} \left| f^t_{01;\frac{1}{2}\frac{1}{2}} + f^t_{01;-\frac{1}{2}-\frac{1}{2}} \right|^2 + \left| f^t_{01;\frac{1}{2}\frac{1}{2}} - f^t_{01;-\frac{1}{2}-\frac{1}{2}} \right|^2 \\ + \left| f^t_{01;\frac{1}{2}-\frac{1}{2}} + f^t_{01;-\frac{1}{2}\frac{1}{2}} \right|^2 + \left| f^t_{01;\frac{1}{2}-\frac{1}{2}} - f^t_{01;-\frac{1}{2}\frac{1}{2}} \right|^2 \end{array} \right\} \qquad (V.9)$$

Most of the t-dependence of $d\sigma/d\Omega$ near $t = 0$ should be determined by the half-angle factors $(\sin\theta_t/2)^{|\lambda-\mu|}(\cos\theta_t/2)^{|\lambda+\mu|}$, the kinematic factors $K(t)$, and the extra zeros which appear in certain $\tilde{f}^t$ in the absence of conspiracy. The remaining factors in $\tilde{f}^t$ are dynamical and are expected to vary only slowly at small t [one would

expect the pion exchange pole to provide an exception, but because $|\mu| = 1$, the pion pole $(\sin \pi \alpha_\pi)^{-1}$ is cancelled in $\tilde{f}^t$ by a factor α_π (see Appendix C). Thus, all $\tilde{f}^t$ are smooth functions below the 2π threshold at $t = 4m_\pi^2$.]

In order to study the difference in t-dependence between the situations with and without conspiracy, then, we approximate the dynamical factors by constants at small t. With this approximation, the helicity amplitudes $\bar{f}^t$ take the forms listed in Table V.3(a). Relating $\bar{f}^t$ to f^t and squaring, we obtain the contributions to $d\sigma/d\Omega$ (V.9) given in the right-hand columns of Table V.3(a). In Table V.3(b) the variation of these contributions at the sample energy $k_\gamma = 3$ BeV/c is indicated by a numerical evaluation at $t = -0.02$ BeV^2 (i.e., a point outside the dip region), $t = -0.003$ BeV^2 (i.e., at center-of-mass angle $\theta_s = 2.8^\circ$, which is near the most forward point measured at present), and $t = t_{min}$ (where $\theta_s = 0^\circ$).

The numerical evaluation at $k_\gamma = 3$ BeV/c works out as follows. In the absence of conspiracy, all kinematic factors in Table V.3 (i, ii, iii, iv, and v) tend to decrease from $t = -0.02$ to $t = -0.003$, which corresponds to the most forward region measured by Buschhorn et al.[59] The decrease by a factor of 100 between $t = .003$ BeV^2 and $t_{min} \approx 0$ is even more striking. Thus, in the absence of conspiracy, there should be a sharp drop in $d\sigma/d\Omega$ in the forward direction (θ less than 2.5° in the center of mass). This drop is already well-known for pion exchange, and our derivation shows it occurs independently of the particle exchanged.

Table V.3(a)

The low t behavior of each photoproduction helicity amplitude, with and without conspiracy, when the dynamical factors and $(t-4M^2)$ are approximated by constants c_i. The contribution of each helicity amplitude in this approximation to $d\sigma/d\Omega$ [the relation of $\cos\theta_t$ to t is given by $\cos^2\theta_t = t\,(2s+t-2M^2-\mu^2)^2/(t-\mu^2)^2(t-4M^2)$].

Amplitude	Behavior Without Conspiracy	Behavior With Conspiracy	Contribution to $\frac{16\pi^2 s p_i}{p_f}\frac{d\sigma}{d\Omega}$ Without Conspiracy	With Conspiracy
$\bar{f}^t_{01;\frac{1}{2}\frac{1}{2}} + \bar{f}^t_{01;-\frac{1}{2}-\frac{1}{2}}$	$c_1\,(t-\mu^2)$	$c_1\,(t-\mu^2)$	$\frac{\lvert c_1\rvert^2}{4}(t-\mu^2)^2\sin^2\theta_t$	$\frac{\lvert c_1\rvert^2}{4}(t-\mu^2)^2\sin^2\theta_t$
$\bar{f}^t_{01;\frac{1}{2}\frac{1}{2}} - \bar{f}^t_{01;-\frac{1}{2}-\frac{1}{2}}$	$c_2\sqrt{t}$	$c_2/\sqrt{t}$	$\frac{\lvert c_2\rvert^2}{4}t\sin^2\theta_t$	$\frac{\lvert c_2\rvert^2}{4t}\sin^2\theta_t$
$\bar{f}^t_{01;\frac{1}{2}-\frac{1}{2}} + \bar{f}^t_{01;-\frac{1}{2}\frac{1}{2}}$	$c_3\sqrt{t}\,(t-\mu^2)$	$\frac{c_3\,(t-\mu^2)}{\sqrt{t}}$	$\frac{\lvert c_3\rvert^2}{4}t(t-\mu^2)^2[1+\cos^2\theta_t] + \frac{\lvert c_4\rvert^2}{4}[1+\cos^2\theta_t]$	$\frac{\lvert c_3\rvert^2}{4t}(t-\mu^2)^2[1+\cos^2\theta_t] + \frac{\lvert c_4\rvert^2}{4}[1+\cos^2\theta_t]$
$\bar{f}^t_{01;\frac{1}{2}-\frac{1}{2}} - \bar{f}^t_{01;-\frac{1}{2}\frac{1}{2}}$	c_4	c_4	$-\mathrm{Re}\,c_3^*\,c_4\,t^{\frac{1}{2}}(t-\mu^2)\cos\theta_t$	$-\frac{\mathrm{Re}\,c_3^*\,c_4}{t^{\frac{1}{2}}}(t-\mu^2)\cos\theta_t$

Table V.3(b)

Sample Values of Kinematic Factors for k_γ = 3 BeV/c

	Factor	t=-0.02 BeV^2	t=-0.003 BeV^2 (2.8° cm)	t = t_{min} (0° cm)
i)	$-(t-\mu^2)^2 \sin^2\theta_t$	0.72 BeV^4	0.11 BeV^4	0
ii)	$t \sin^2\theta_t$	9.2 BeV^2	0.64 BeV^2	0
ii)'	$\sin^2\theta_t/t$	2.3×10^4 BeV^{-2}	7.1×10^4 BeV^{-2}	0
iii)	$-t\,(t-\mu^2)^2\,[1+\cos^2\theta_t]$	1.4×10^{-2} BeV^6	3.3×10^{-4} BeV^6	7.8×10^{-9} BeV^6
iii)'	$-\frac{1}{t}\,(t-\mu^2)^2\,[1+\cos^2\theta_t]$	36.1 BeV^2	36.2 BeV^2	72 BeV^2
iv)	$[1+\cos^2\theta_t]$	460	214	2
v)	$\lvert t^{\frac{1}{2}}\,(t-\mu^2)\cos\theta_t\rvert$	1.2×10^{-1} BeV^3	1.8×10^{-2} BeV^3	6.6×10^{-5} BeV^3
v)'	$\lvert\frac{1}{t^{\frac{1}{2}}}\,(t-\mu^2)\cos\theta_t\rvert$	6 BeV	6 BeV	6 BeV

Kinematic factors (ii)', (iii)', and (v)', which replace (ii), (iii), and (v) in the presence of conspiracy, tend to show the forward rise indicated by experiment as θ_{CM} decreases to 2.5^{o}. At still smaller angles, the difference between the cases with and without conspiracy become more dramatic; (v)' is constant, (iii)' remains essentially constant from $\theta_{CM} = 2.5$ to $\theta_{CM} = 0.5^{o}$ before doubling at $\theta_{CM} = 0^{o}$, and (ii)' remains essentially constant from $\theta_{CM} = 2.5^{o}$ to $\theta_{CM} = 0.5^{o}$ before plunging to zero at $\theta_{CM} = 0^{o}$. Thus the deep forward dip predicted by standard techniques for reggeizing individual exchanges should be absent if conspiring trajectories dominate the cross section.[62]

The same qualitative features apply at energies below 3 BeV. While the dip which distinguishes the no-conspiracy from the conspiracy case becomes less striking at low energies, the depth being of order $10\ (E_{\gamma}/\text{BeV})^{2}$, the effect persists below 1 BeV.[63] Thus, for example, the measurements at $E_{\gamma} = 800$ MeV by Beneventano et al.,[59] who find $d\sigma/d\Omega$ rising as θ_{CM} is decreased by steps of 2^{o} from 10^{o} to 0^{o}, are relevant and strongly favor conspiracy. The measurements down to 5^{o} by Ecklund and Walker at somewhat higher energies, and down to 2.5^{o} by Buschhorn et al. at 1.2 to 2.9 BeV, support the same conclusion. If this pattern is corroborated by extension of the higher energy measurements to 0^{o}, the existence of conspiracy will be firmly established.[64]

It should perhaps be emphasized that the expansion of the differential cross section in terms of t-channel amplitudes is correct at all energies, as is the assignment of kinematic factors to the t-channel amplitudes. Thus the above discussion depends in no way

upon conspiracy between Regge trajectories; it requires only conspiracy between t-channel amplitudes. As mentioned above, a conspiracy of exactly this type is provided by the s-channel nucleon pole in Born approximation[57]; likewise the "absorptive corrections" to one pion exchange, which are made by adding several low partial waves in the direct channel, remove the dip which the unmodified one pion exchange would exhibit at $t = 0$. It is therefore entirely possible that the exciting possibility of conspiracy between trajectories is not realized in $\gamma p \to \pi^+ n$, and that the conspiracy indicated by experiment is just an old theory in disguise.

CONCLUSIONS

This study indicates that the experimental differential cross sections and density matrices of reactions of the form $\pi N \rightarrow VN$, $\pi N \rightarrow V\Delta$ can be understood on the basis of a Regge pole model provided:

a) The half-angle factors in t-channel amplitudes are treated as kinematic factors and evaluated explicitly.

b) The results of Freedman and Wang[1] are assumed to apply to the regularized t-channel parity-conserving helicity amplitudes.

c) Kinematic constraint equations at thresholds and pseudothresholds are taken into account, where necessary.

d) The contraint equations at $t = 0$ (conspiracy equations) are satisfied by evasion, at least for the dominant exchanges.

Further, the data seem to indicate that the residue functions are approximately constant once kinematic behavior has been removed.

This model cannot explain presently available photoproduction data. Published results and preliminary data at very small t indicate that conspiracy between helicity amplitudes occurs in this case. It is not clear whether the data can be explained solely by Regge pole exchange; other singularities in the angular momentum plane may have to be invoked.

APPENDIX A

Cohen-Tannoudji et al., found that in reactions (such as $\pi N \to V\Delta$) with unequal masses in both t-channel states, the technique described in Section 2.2 does not lead to any conspiracy relations between different $\bar{f}^t_{cd;ab}$'s. It does, however, lead to relations between different parity-conserving amplitudes.[65] If the amplitudes are dominated by Regge poles, different poles will dominate different parity-conserving amplitudes; thus the relations obtained are of a non-trivial nature. For this reason the simple derivation is presented in detail.

For each individual amplitude $\bar{f}^t_{cd;ab}$ in reactions where the masses are related as in $\pi N \to V\Delta$, the Wang kinematic factor at $t = 0$ allows a maximum singularity $(1/\sqrt{t})^{|\lambda-\mu|}$, where $\lambda = a-b$, $\mu = c-d$. Thus $\bar{f}^t_{cd;ab}$ and $\bar{f}^t_{-c-d;ab}$ have different maximum singularities unless at least one of μ and λ vanishes. The parity-conserving combinations $(\bar{f}^t_{cd;ab} \pm \bar{f}^t_{-c-d;ab})$ are allowed the larger of the two singularities, i.e., $(1/\sqrt{t})^{(|\lambda|+|\mu|)}$. Hence if $P = ||\mu|-|\lambda||$, $Q = |\mu|+|\lambda|$ and $\bar{f}^t_{cd;ab}$ is the individual amplitude which is only allowed the smaller singularity, we have

$$\bar{f}^t_{cd;ab} \sim (1/\sqrt{t})^P \tag{A.1}$$

and

$$\bar{f}^t_{cd;ab} = \tfrac{1}{2}\left[(\bar{f}^t_{cd;ab} + \bar{f}^t_{-c-d;ab}) + (\bar{f}^t_{cd;ab} - \bar{f}^t_{-c-d;ab})\right] \tag{A.2}$$

$$\sim \tfrac{1}{2}\left[\frac{C_1}{(\sqrt{t})^Q} + \frac{C_2}{(\sqrt{t})^Q}\right]$$

To make (A.2) consistent with (A.1), $C_1 + C_2$ must have a zero of order $(\sqrt{t})^{Q-P}$ at $t = 0$. As with all $t = 0$ constraint equations this can either be satisfied by conspiracy (C_1 and C_2 non-vanishing and correlated) or non-conspiracy (C_1 and C_2 separately vanishing like $(\sqrt{t})^{Q-P}$).[66]

This derivation does not make explicit use of the crossing matrix, but it is easy to verify that conditions of type (II.23) do arise if one works with parity-conserving amplitudes, and lead to the same $t = 0$ relations as described above.

As a particularly simple example of this type of conspiracy, consider the s-channel reaction $\pi\pi \to \gamma\gamma$. The relations can be derived as in Equations (A.1 - A.2), or from the invariant amplitudes for this case., but it is instructive to work through the crossing method of Cohen-Tannoudji et al. The crossing relations for the helicity amplitudes are

$$\begin{aligned} f^t_{+0;+0} &= f^s_{+\ -;00} \\ f^t_{+0;-0} &= f^s_{++;00} \end{aligned} \tag{A.3}$$

Rewriting Equation (A.3) in terms of $\bar{f}$'s one finds

$$\begin{aligned} \bar{f}^t_{+0;+0} &= \frac{(\sin\theta_s)^2}{4\,(\cos\theta_t/2)^2}\ \bar{f}^s_{+\ -;00} \\ \bar{f}^t_{+0;-0} &= \frac{1}{(\sin\theta_t/2)^2}\ \bar{f}^s_{++;00} \end{aligned} \tag{A.4}$$

which can be re-expressed in terms of s and t:

$$\bar{f}^t_{+0;+0} = \frac{-(t-\mu^2)^2}{4s(s-4\mu^2)} \bar{f}^s_{+-;00}$$

$$\bar{f}^t_{+0;-0} = \frac{-(t-\mu^2)^2}{st} \bar{f}^s_{++;00} \qquad \text{(A.5)}$$

By standard reasoning,[2,8] the $\bar{f}^s$ have no kinematic singularities or zeros in t. Thus it follows from the crossing relations (A.5) that $\bar{f}^t_{+0;+0} \sim$ constant at t = 0 and $\bar{f}^t_{+0;-0} \sim t^{-1}$. The amplitudes

$$a = -\frac{1}{(t-\mu^2)^2} \bar{f}^t_{+0;+0}$$

$$b = -\frac{t}{(t-\mu^2)^2} \bar{f}^t_{+0;-0} \qquad \text{(A.6)}$$

are therefore free of kinematic singularities of zeros at t = 0.[67] The counterpart of Equation (II.21) for this case is

$$\begin{pmatrix} \bar{f}^s_{+-;00} \\ \bar{f}^s_{++;00} \end{pmatrix} = \begin{pmatrix} 4s\,(s-4\mu^2) & 0 \\ 0 & s \end{pmatrix} \begin{pmatrix} a \\ b \end{pmatrix} \qquad \text{(A.7)}$$

which, analyzed by the procedure of Equations (II.22-23) gives no t = 0 relations. This is in agreement with the conclusions of Cohen-Tannoudji et al. about the lack of conspiracy between different $\bar{f}^t_{cd;ab}$'s. But if we turn to parity-conserving combinations

$(\bar{f}^t_{+0;+0} + \bar{f}^t_{-0;+0})$ and $(\bar{f}^t_{+0;+0} - \bar{f}^t_{-0;+0})$, the reasoning following Equation (A.5) indicates that both parity-conserving amplitudes $\sim t^{-1}$ at $t = 0$, and that in this case the amplitudes which are free of kinematic singularities or zeros at $t = 0$ can be written[68)]

$$\begin{aligned} \tilde{f}^{t(+)}_{+0;+0} &= \frac{t}{(t-\mu^2)^2} \left(\bar{f}^t_{+0;+0} + \bar{f}^t_{-0;+0}\right) \\ \tilde{f}^{t(-)}_{+0;+0} &= \frac{t}{(t-\mu^2)^2} \left(\bar{f}^t_{+0;+0} - \bar{f}^t_{-0;+0}\right) \end{aligned} \tag{A.8}$$

(note that $\bar{f}^t_{-0;+0} = \bar{f}^t_{+0;-0}$).

Working out the crossing matrix connecting $\tilde{f}^t$ to $\bar{f}^s$, we find

$$\begin{pmatrix} \bar{f}^s_{+-;00} \\ \\ \bar{f}^s_{++;00} \end{pmatrix} = \begin{pmatrix} \frac{-2s\ (s-4\mu^2)}{t} & \frac{-2s(s-4\mu^2)}{t} \\ \\ -s/2 & s/2 \end{pmatrix} \begin{pmatrix} \tilde{f}^{t(+)}_{+0;+0} \\ \\ \tilde{f}^{t(-)}_{+0;+0} \end{pmatrix} \tag{A.9}$$

For this matrix, the procedure of Equations (II.21-23) gives the condition

$$t\left[\bar{f}^t_{+0;+0} + \bar{f}^t_{-0;+0}\right] = -t\left[\bar{f}^t_{+0;+0} - \bar{f}^t_{-0;+0}\right] \tag{A.10}$$

at $t = 0$. As usual this relation can be satisfied either by separate zeros in both parity-conserving amplitudes, or by conspiracy between them.

APPENDIX B

Crossing Relations in the Forward Direction For Unequal Mass Reactions

The Trueman-Wick[9] crossing relations between t-channel and s-channel helicity amplitudes may be put in the form[2]

$$f^{t}_{cd;ab} = \sum d^{J_a}_{A'a}(\chi_a)\, d^{J_b}_{b'b}(\chi_b)\, d^{J_c}_{c'c}(\chi_c)\, d^{J_d}_{D'd}(\chi_d)\, f^{s}_{c'A';D'b'} \tag{B.1}$$

where

$$\sin\chi_a = \frac{2\, m_a \sqrt{\varphi(s,t)}}{t_{ab}\, s_{ac}} \qquad \sin\chi_c = \frac{2\, m_c \sqrt{\varphi(s,t)}}{t_{cd}\, s_{ac}}$$

$$\sin\chi_b = \frac{2\, m_b \sqrt{\varphi(s,t)}}{t_{ab}\, s_{bd}} \qquad \sin\chi_d = \frac{2\, m_d \sqrt{\varphi(s,t)}}{t_{cd}\, s_{bd}} \tag{B.2}$$

$$t_{ij} = \left[t - (m_i + m_j)^2\right]^{\frac{1}{2}} \left[t - (m_i - m_j)^2\right]^{\frac{1}{2}}$$

$$s_{ij} = \left[s - (m_i + m_j)^2\right]^{\frac{1}{2}} \left[s - (m_i - m_j)^2\right]^{\frac{1}{2}} \tag{B.3}$$

$$\begin{aligned}\varphi(s,t) = {} & st\,(\Sigma\, m_i^2 - s - t) - t\,(m_b^2 - m_d^2)(m_a^2 - m_c^2) \\ & - s\,(m_a^2 - m_b^2)(m_c^2 - m_d^2) \\ & - (m_a^2\, m_d^2 - m_c^2\, m_b^2)\,(m_a^2 + m_b^2 + m_c^2 + m_d^2)\end{aligned} \tag{B.4}$$

and φ vanishes on the boundary of the physical region.

For those cases where the masses are unequal in either the final or the initial state of the t-channel, $\varphi = 0$ does not coincide with $t = 0$ at finite s. At $\varphi = 0$, therefore, the sines of all the crossing angles vanish; hence, these angles must assume the values 0 or π. When these values are substituted into the crossing matrix, it is easily seen that each s-channel helicity amplitude crosses to only one t-channel amplitude along the curve $\varphi = 0$, and that this crossing is such that each helicity index in the amplitude either remains the same or changes sign.

It has been shown by Shepard[69] that a) for the particles at a t-channel vertex connecting unequal non-zero masses, both helicities flip (don't flip) if the mass of the particle whose line is reversed under crossing is less (greater) than the mass of the uncrossed particle; b) at a vertex connecting equal non-zero masses, both helicities flip (don't flip) if (for the unequal mass pair at the other vertex) the mass of the particle which gets crossed is greater (less) than the mass of the uncrossed particle. Hence for the s-channel reactions $\pi N \to VN$ and $\pi N \to V\Delta$ the crossing relations along the curve $\varphi = 0$ take the form

$$f^{t}_{co;ab} = \pm f^{s}_{-ca;ob} \qquad (B.5)$$

APPENDIX C

Kinematic Singularities and External Photons

The K listed in Table V.1 were obtained by taking the comparable factors from the amplitudes for $\pi B \to VB$ and forming $\lim_{m_V \to 0} K$. Note that two of the K in Table I contain a factor $(t-\mu^2)$ and the other two do not.

Study of the explicit crossing matrix for photoproduction evaluated directly at $m_\gamma = 0$, on the other hand, gives a factor $(t-\mu^2)$ in the K for <u>all four</u> helicity amplitudes. An analogous discrepancy has been found by Horn[67] in the reaction $\gamma\gamma \to \pi\pi$. Thus the determination of kinematic singularities from crossing matrix considerations must be re-examined when one or more of the external particles has zero mass.

In order to decide which prescription for K is more suitable -- the limit as $m_V \to 0$ of K calculated from the crossing matrix for $m_V \neq 0$, or K calculated directly from the crossing matrix for $m_V = 0$ -- let us turn to the reggeization of pion exchange. If we reggeize parity-conserving helicity amplitudes in the manner discussed in Chapter 2, the dynamical pion pole contributes only to the particular parity-conserving amplitude

$$\bar{f}^t_{01;\frac{1}{2}\,\frac{1}{2}} - \bar{f}^t_{01;-\frac{1}{2}\,-\frac{1}{2}} = \Sigma\ (2J+1)\ b_J^-(t)\ P^{(1,1)}_{J-1}(\cos\theta_t)\ .$$

Because reggeization of $P_{J-1}^{(1,1)}(x)$ leads to a term proportional to $\alpha_s^{\alpha-1}$, the contribution of pion trajectory exchange to amplitudes $f^t_{01;\frac{1}{2}\frac{1}{2}}$ and $f^t_{01;-\frac{1}{2}-\frac{1}{2}}$ assumes the form

$$f^t_{01;\lambda_1\lambda_1} \to (\sin\theta_t/2)(\cos\theta_t/2)\frac{\sqrt{t-4M^2}}{\sqrt{t}}\ \frac{\gamma(t)\ \alpha_s^{\alpha-1}\ (1+e^{-i\pi\alpha})}{\sin\pi\alpha}$$

where we have inserted K(t) from Table V.1. As first noticed by Zweig,[70] the pion pole in this expression emerges in a curious way. The dynamical contribution is proportional to $\alpha_\pi/\sin\pi\alpha_\pi$, which contains no pole at $\alpha_\pi = 0$. However, the kinematic factor

$$2\sin\frac{\theta_t}{2}\cos\frac{\theta_t}{2} = \sin\theta_t = \sqrt{1-\cos^2\theta_t}$$

introduces a pole at $t = \mu^2$ because

$$\cos^2\theta_t = t\,[2s + t - 2M^2 - \mu^2]^2\ (t-4M^2)^{-1}\ (t-\mu^2)^{-2}\ .$$

Thus the pion pole arises kinematically when the K of Table V.1 is used.

The alternative K, obtained by working directly with the crossing matrix at $m_\gamma = 0$, has an additional factor $t-\mu^2$. If this K were used in the above formalism, it would cancel the $t=\mu^2$ pole from the half-angle factors, and the resulting amplitude would have no pion pole. This would contradict gauge invariant perturbation theory, where f^t does have a pion pole, and the experimental observation that such a pole is necessary to fit charged photoproduction data. Hence,

we feel that the K listed in Table V.1 are to be preferred.[71].

When the kinematic factor listed in Table V.1 is used for a <u>non-pion</u> $P = (-1)^{J+1}$ exchange, a spurious pole at $t = \mu^2$ will appear. Residues of these exchanges should include a dynamic zero of form $q.K = \frac{(t-\mu^2)}{2}$ to cancel this pole.[72]

REFERENCES

1. D. Freedman and J-M. Wang, Phys. Rev. Letters 17, 569 (1966).

2. Ling-Lie Wang, Phys. Rev. 142, 1187 (1966).

3. Ling-Lie Wang, Phys. Rev. 153, 1664 (1967).

4. G. Cohen-Tannoudji, A. Morel, and H. Navelet, "Kinematical Singularities, Crossing Matrix, and Kinematical Constraints for Two-Body Helicity Amplitudes", Saclay preprint (1967).

5. M. Gell-Mann, M. Goldberger, F. Low, E. Marx, and F. Zachariasen, Phys. Rev. 133, B145 (1964).

6. M. Jacob and G.C. Wick, Ann. Phys. 7, 404 (1959).

7. In particular, the Jacobi polynomials are finite and non-zero at $\cos \theta_t = \pm 1$, which ensures that the half angle factors in Eq. (II.13) contain just the right number of zeros at these points.

8. Y. Hara, Phys. Rev. 136, B507 (1964).

9. T.L. Trueman and G.C. Wick, Ann. Phys. 26, 322 (1964).

10. G.C. Fox, Phys. Rev. 157, 1493 (1967).

11. B. Diu and M. Le Bellac, "Kinematical Constraints on Regge Pole Residues", Orsay preprint (1967).

12. Special considerations are also required for reactions involving photons; see Chapter 5.

13. No inverse of $\tilde{X}$ is required since $\tilde{X}^{-1}$ is known directly from the crossing relation between $\tilde{f}^t$ and $\bar{f}^s$.

14. According to an investigation by Frank Henyey (private communication), if $\tilde{X}$ is defined as in Eq. (II.20), det $\tilde{X}$ has three zeros at $t = 4M^2$. These three zeros provide the amplitude for $({}^3J + 1_J \to {}^3J + 1_J)$ with an additional factor $q_t{}^4 \sim (t - 4M^2)^2$, and the amplitude for $({}^3J + 1_J \to {}^3J - 1_J)$ with an additional factor $q_t{}^2$, relative to the amplitude for $({}^3J - 1_J \to {}^3J - 1_J)$.
   The determinant of the crossing matrix connecting the amplitudes used by Wang in Ref. 2, Section IV-A, has two further zeros. The additional two zeros arise because Wang has not used "parity-conserving" helicity amplitudes at this point; alternatively, they can be viewed as providing each of the ${}^1J_J$ and ${}^3J_J$ amplitudes with a threshold factor $q_t{}^2$ relative to the amplitude for $({}^3J - 1_J \to {}^3J - 1_J)$.

15. K. Bardakci and G. Segré, "Some Conspiracy and Superconvergence Properties of Scattering Amplitudes in the Helicity Formalism",

Berkeley preprint (1967).

16. A more general discussion of spin-parity combinations for which this sort of restriction on M occurs can be found in Ref. 3, Appendix 3.

17. S-U. Chung et al., Phys. Rev. Letters 16, 481 (1966).

18. An estimate of the region in which suppression is most important may be obtained by at least two methods:
i) Calculate $\cos^2\theta_t$ for the s in question as a function of t. It is found that it rises sharply from 1 at t_{min} to some $(\cos^2\theta_t)_0$, and then remains close to this value for the rest of the range considered, ($|t| \leq 0.5$ GeV^2). The rise for $2.5 \leq P_\pi \leq 8$ GeV/c occurs principally in region $|t| \leq 0.2$ GeV^2.

ii) Calculate $(d \cos\theta_t)/ds$ as a function of t. This increases rapidly from θ at $t = 0$ as $|t|$ increases in the physical region. Above $|t| \approx 0.2$ GeV^2, the rate of increase $\left(\frac{d}{d(-t)} \frac{d}{ds} (\cos\theta_t) \right)$ is appreciably slower than it is below this value. This criterion depends only on the masses involved -- not on the energy of the experiment.

19. This is the one place in the present section where the nearness of the pi pole is brought in explicitly.

20. This has also been noticed by B. Diu and M. Le Bellac, Physics Letters 24B, 416 (1967).

21. The unexpected $t^{-1/2}$ for $P = (-1)^{J+1}$, $\mu = 0$, $\lambda = 1$ can be obtained from the amplitude $\epsilon^\mu \bar{N} \gamma_5 \gamma_\mu N$ by remembering that the longitudinal ϵ^μ vector is singular at $t = 0$ for this problem[8]

$$\epsilon_0^{\ \mu} = \frac{1}{m_\rho} \ (P_\rho; \ P_\rho^{\ 0} \hat{P}_\rho)$$

As the contribution of this amplitude to the cross section must vanish in the forward direction ($t = t_{min} \neq 0$) due to angular momentum conservation, the presence or absence of this $1/\sqrt{t}$ is not of major importance to the effect discussed here. It should be noted, however, that if only the amplitude $f^t_{00;1/2-1/2}$ is excited (corresponding to standard treatment of a single Regge pole exchange with the appropriate quantum numbers), a thorough study of subsidiary conditions at $t = 0$[53] requires that $f^t_{00;1/2-1/2}$ behave like $\sqrt{t}$ rather than like $1/\sqrt{t}$; this further suppresses it in the forward direction (see also Chapter 4).

22. R. George et al., Nuovo Cimento 46, 539 (1966) and CERN preprint 66-18.

23. British-German collaboration, Phys. Rev. 138, B897 (1965).

24. Aachen, Physics Letters 19, 609 (1965).

25. D.H. Miller et al., Phys. Rev. 153, 1423 (1967).

26. An additional indication of the nature of the exchanges is the zero in ω exchange at $\alpha = 0$, $t \approx -0.5$ GeV^2. If ω exchange is important, this should produce a sharp dip in the cross section at this point. Because the relative importance of ω exchange at this t is expected to increase with energy, the dip should become more prominent as s increases. So far, a dip at this place has been observed only in $\pi^+p \to \rho^+p$ at 4 GeV/c [23].

27. H. Cohn, W. Bugg, and G. Condo, Physics Letters 15, 344 (1965).

28. Ling-Lie Wang, Phys. Rev. Letters 16, 756 (1966).

29. R. Dashen and S.C. Frautschi, Phys. Rev. 152, 1450 (1966).

30. L. Stodolsky and J. Sakurai, Phys. Rev. Letters 11, 90 (1963).

31. British-German collaboration, Nuovo Cimento 35, 659 (1965).

32. M. Barmawi, Phys. Rev. 142, 1088 (1966), and Phys. Rev. Letters 16, 595 (1966). To obtain a rough estimate of the position of the B trajectory, assume that it is a straight line with a slope of 1. In order that it assume the value + 1 at $t = (1.22)^2$ GeV^2, α_B must be $t - 0.49$. Recent fits to the ρ trajectory give $\alpha_\rho \approx t + 0.5$. Hence $\alpha_\rho - 1 \lesssim \alpha_B$ and the ρ and B contributions will have similar s-dependence in the low t region.

33. K. Gottfried and J.D. Jackson, Nuovo Cimento 33, 309 (1964).

34. J. Friedman and R. Ross, Phys. Rev. Letters 16, 485 (1966).

35. If a particular model is so restrictive that the cross sections drop in the forward direction like $\sin^2\theta_t$, the predicted shapes at $t = 0$ of some of the density matrix elements will be different from those in Table III.2. Experimental cross sections do not seem to have this sort of behavior.

36. J.D. Jackson et al., Phys. Rev. 139, B428 (1965).

37. British-German collaboration, Nuovo Cimento 31, 734 (1964).

38. R. Thews, Phys. Rev. 155, 1624 (1967).

39. P.C.M. Yock and D. Gordon, Phys. Rev. 157, 1362 (1967).

40. For amplitudes with $\lambda \neq 0$, $\mu \neq 0$, the combination $\bar{f}^t_{cd,ab} \pm \bar{f}^t_{-c-d,ab}$ no longer couples to definite parity states ($P = (-1)^J$ or $(-1)^{J+1}$), so the argument might appear to lose force. But for each ℓ the highest power of $\cos\theta_t$ in P_{J-M} still has a definite parity, and it is the highest power which gives the controlling singularity.

41. See also H.F. Jones, "Threshold Conditions for Helicity Amplitudes", Imperial College, London preprint (1966).

42. Except for $J^P = 1^+$ at $t = (M_\Delta + M_N)^2$, where $\ell = 1$ is the lowest one can reach.

43. D. Brown et al., UCRL-17665.

44. I am indebted to M. Le Bellac and J.D. Jackson for bringing this fact to my attention.

45. W.L. Yen et al., Phys. Rev. Letters 18, 1091 (1967).

46. L.D. Jacobs, Ph.D. Thesis (UCRL report 16877), p. 145 (1966).

47. CERN-Brussels collaboration, Nuovo Cimento 46A, 593 (1966); and Y. Goldschmidt-Clermont, private communication.

48. F. Bruyant et al., International Conference on High-Energy Physics, Dubna 1, 422 (1964).

49. M. Wahlig et al., Phys. Rev. 147, 941 (1966).

50. S. Mandelstam, Nuovo Cimento 30, 1113 and 1127 (1963).

51. Y. Hara, Phys. Rev. 140, B178 and B1649 (1965).

52. Lorella Jones, "Information about Regge Pole Couplings from Vector Meson Production". CALT-68-125 (1967).

53. H. Hogaasen and Ph. Salin, "General Classification of Conspiracy Relations", CERN preprint TH.788

54. M.B. Halpern, Institute for Advanced Study preprint, "Conspiracy and Superconvergence in Pion Photoproduction", (1967).

55. J.S. Ball, Phys. Rev. 124, 2014 (1961).

56. S.L. Adler and F.J. Gilman, Phys. Rev. 152, 1460 (1966).

57. Evaluation of the nucleon pole diagram for this process gives

$$\bar{f}^t_{01;-+} + \bar{f}^t_{01;+-} = \frac{(t - \mu^2)\sqrt{2}}{\sqrt{t}} \quad \frac{1}{(s - M^2)}$$

$$\bar{f}^t_{01;++} - \bar{f}^t_{01;--} = \frac{1}{\sqrt{2}} \quad \frac{(t + \mu^2)\sqrt{t - 4M^2}}{\sqrt{t} \quad M \quad (s - M^2)}$$

which satisfy Eq. (V.1).

58. This point has also been realized by S. Drell and J. Sullivan, Phys. Rev. Letters 19, 268 (1967).

59. M. Beneventano et al., Nuovo Cimento 28, 1464 (1963);
S.D. Ecklund and R.L. Walker, Phys. Rev. 159, 1195 (1967);
G. Buschhorn et al., Phys. Rev. Letters 18, 571 (1967).

60. P.K. Mitter, "O(4) Symmetry and the Forward Photoproduction of Pions at High Energies", U.C. Santa Barbara preprint (1967).

61. R.F. Sawyer, "Forward Peaks from the Exchange of Odd Parity Regge Trajectories", U.C. Santa Barbara preprint, (1967).

62. Of course, conspiracy does permit some decrease of the forward cross section if the Regge α has a special value such that the c_2 term dominates c_3 and c_4, or c_3 and c_4 have a strong destructive interference.

63. Note that no high-energy approximation has been made in Table V.3(a).

64. In this section we have compared the behavior when all trajectories conspire, and when no trajectories conspire. Most likely, however, the actual situation is mixed - some trajectories conspiring, others not. If this is the case and if the highest ranking trajectory which contributes does not conspire, a forward dip will eventually develop when experiments reach sufficiently high energies. Unless the first conspiring trajectory is a whole unit of angular momentum down, the cross section will dip only to the level of the conspiring trajectories instead of falling as far as indicated in Table V.3.

65. These appear to be the same relations derived by Toller from group theoretical considerations: M. Toller, "Some Consequences of a Generalization of the Regge Pole Hypothesis", Rome preprint (1967).

66. Note that the property $\bar{f}^t_{cd;ab} \sim (\pm)\ \bar{f}^t_{-c-d;ab}$, which holds for the contribution of a Regge pole of definite parity to the amplitude at asymptotically large s, is consistent with the singularities at t = 0 only if the no conspiracy choice

$$\bar{f}^t_{cd;ab} \sim \left(\frac{1}{\sqrt{t}}\right)^P \qquad \bar{f}^t_{-c-d;ab} \sim \left(\frac{1}{\sqrt{t}}\right)^P$$

is made. This is not surprising since, as explained above, the conspiracies in these amplitudes are necessarily between trajectories of opposite parity .

67. D. Horn, Caltech Report CALT-68-131/Internal Report 34(1967).

68. As described in Appendix C, reactions with photons have special features, and other arguments give $\tilde{f}^t$ a different factor at $t = \mu^2$. However, this does not affect the discussion of behavior at t = 0.

69. H. Shepard, Phys. Rev. 159, 1331 (1967).

70. G. Zweig, Nuovo Cimento 32, 689 (1964).

71. In other words, if one uses the other K_2 a kinematic pole must be inserted at $t = \mu^2$ in the resulting f, in order to obtain the pion pole observed in nature.

72. Notice that factors of $(t - \mu^2)$ have negligible effect in the extremely low $|t|$ region influenced by conspiracy. Thus this choice of threshold behavior does not affect conclusions about the presence or absence of conspiracy.